# A NOVEL, GREEN TECHNOLOGY FOR THE PRODUCTION OF AROMATIC THIOL FROM AROMATIC SULFONYL CHLORIDE

A Dissertation

by

BRADLEY RUSTON ATKINSON

Submitted to the Office of Graduate Studies of
Texas A&M University
in partial fulfillment of the requirements for the degree of

DOCTOR OF PHILOSOPHY

May 2008

Major Subject: Chemical Engineering

# A NOVEL, GREEN TECHNOLOGY FOR THE PRODUCTION OF AROMATIC THIOL FROM AROMATIC SULFONYL CHLORIDE

A Dissertation

by

BRADLEY RUSTON ATKINSON

Submitted to the Office of Graduate Studies of
Texas A&M University
in partial fulfillment of the requirements for the degree of

DOCTOR OF PHILOSOPHY

Approved by:

| | |
|---|---|
| Chair of Committee, | Rayford G. Anthony |
| Committee Members, | Mahmoud El-Halwagi |
| | Perla Balbuena |
| | Lisa Perez |
| Head of Department, | Michael Pishko |

May 2008

Major Subject: Chemical Engineering

# ABSTRACT

A Novel, Green Technology for the Production of Aromatic Thiol from Aromatic Sulfonyl Chloride. (May 2008)

Bradley Ruston Atkinson, B.S., University of Arkansas; M.S., University of Arkansas

Chair of Advisory Committee: Dr. Rayford G. Anthony

The hydrogenation of aromatic sulfonyl chloride to produce aromatic thiol is an important industrial reaction. The aromatic thiol is a critical intermediate in the production of many pharmaceuticals as well as several agrochemicals. Density Functional Theory (DFT), a quantum mechanical method, was used to investigate the new aromatic thiol production technology at the molecular level in aspects including reaction species adsorption and transition state determination. Plant design methods and economic analysis were performed to determine the economic feasibility of the new technology in the current specialty chemicals market.

The quantum mechanical calculations showed that the molecules adsorbed to three simulated (100) Pd catalyst surfaces will preferentially move to configurations that are favorable for reaction progression. The calculations also show that the proposed reaction sequence by DuPont is the most feasible option despite the investigation into an alternative sequence that arose from molecular observations during calculations. Predicted activation energies (Ea) were in the range of 6.88 – 38.1 kcal/mol which is

comparable to the 14.58 kcal/mol determined experimentally by DuPont, and the differences between experimental and simulated values are easily explained.

Plant design calculations show that a semi-batch reactor plant can easily produce 2MM lb of thiol/year, giving the owner of the plant an immediate 18% market share in the worldwide market of benzenethiol. Economic analysis shows that a grassroots plant construction is not currently an economically feasible option for corporate investment unless a source of cheap, skilled labor can be found in addition to a means of a 25% discount on certain raw material feed stocks. However, if both of these requirements can be fulfilled then new plant construction will have a payback time of 3.71 years based on the price of benzenethiol in the summer of 2007, $2.27/lb thiol.

## ACKNOWLEDGEMENTS

I would like to express my appreciation to my committee chair, Dr. Anthony, and my committee members, Dr. Perez, Dr. Balbuena, and Dr. El-Halwagi, for providing invaluable insight and guidance in the simulation, design and evaluation process. I also appreciate the support of the Laboratory for Molecular Simulation (LMS), Texas A&M University for providing software and guidance for this investigation.

Thanks also go to my friends and colleagues and the department faculty and staff for making my time at Texas A&M University a great experience.

Finally, thanks to my mother, father and the rest of my family for their encouragement and patience.

# TABLE OF CONTENTS

Page

# LIST OF FIGURES

FIGURE Page

FIGURE Page

# LIST OF TABLES

# 1. INTRODUCTION

In the past few decades there has arisen in the chemical industry a dichotomy between synthesizing products for profit and synthesizing products with methods minimizing environmental impact. Numerous governmental agencies have been formed and funded with billions of tax payer dollars for the purpose of regulating chemical manufacturer's effects on the planet. Buzz words and phrases like "Green Chemistry"[1] have been coined and put to good use. Still, in many cases throughout the chemical industry, and particularly in the area of specialty chemicals, the actual chemistry is the same as it has been for 50 to 75 years. The downstream and environmental effects of the profitable reactions are reduced by further processing or by highly regulated waste disposal. All of these additional costs are decreasing industrial profit margins. While these economic losses provide a necessity for invention of novel waste-treating and waste disposal technologies, fewer researchers are looking into changing the underlying chemistries that make the products in the first place.

Texas A&M has acquired the rights to a patent[2] that revises the chemistry for an important fine chemical reaction and makes it more environmentally friendly. This novel process is used for the synthesis of aromatic thiols from aromatic sulfonyl chlorides and it eliminates the need for heavy metal salt processing or disposal completely. Aromatic thiols are of industrial importance due to their use in the manufacture of agrochemicals,

---

This dissertation follows the style of Journal of Molecular Catalysis A: Chemical.

polymers, pigments, dyes and pharmaceuticals.[3,4] The technology takes advantage of a hydrogenation over a palladium on carbon (Pd/C) catalyst to produce the aromatic thiols without the toxic by-products. Being an emergent technology with very little experimental or theoretical data available for research, Texas A&M, and specifically the Kinetics, Catalysis and Reaction Engineering Laboratory (KCRE), has taken on the challenge of investigating this technology for economic, scientific and academic information.

Advancements in understanding surface chemistry and catalysis have been made in many areas using quantum mechanical techniques. These techniques let the researchers experiment theoretically on energy surfaces and electron interactions at the molecular level. They involve solving equations, with a pre-determined set of simplifications and assumptions, for a set of atoms put in place by the experimenter. These simulations generally involve a minimizing of the overall energy of the system by allowing the atoms to move about in accordance with wave theory until the energy of the system comes to a minimum and the displacement of, as well as the forces acting upon, the individual atoms is below a tolerance level. Publications of papers for aromatic molecule to surface interactions over simulated palladium clusters are quite extensive, but none apply directly to the reactions involved in the technology.

The work described herein presents the use of quantum mechanical methods that have been used herein to investigate this novel, green technology for synthesizing aromatic

thiols. Molecule/surface interactions were simulated for all reaction species. Transition states for an initial reaction step were also determined using different simulated Pd/C clusters. The results of these simulations were compared to available experimental data to provide a more detailed view of what is happening within the reactor and, more specifically, on the surface of the catalyst. Basic economic design and analysis for a plant capable of producing 2 million pounds per year (lb/yr) of benzenethiol is also presented. All of this work will lead to a better understanding of the technology on several different fundamental levels and perhaps, eventually, to its commercial utilization in the future.

# 2. LITERATURE REVIEW

## 2.1 - Introduction

Aromatic thiols are of industrial importance due to their use in the manufacture of agrochemicals, polymers, pigments, dyes and pharmaceuticals.[3,4] The possible harmful downstream and environmental effects of these profitable reactions are reduced by further processing or by highly regulated waste disposal. All of these additional costs are decreasing industrial profit margins. While these economic losses provide a necessity for invention of novel waste-treating and waste disposal technologies, fewer researchers are looking into changing the underlying chemistries that make the products in the first place. With the specialty chemicals marketplace expanding worldwide and with more and more chemical producers making specific products for specific clients the need for exposure to specialty chemicals processing extends all the way into the education of undergraduate chemical engineering students. Investigations into the technology discussed here can have practical economic impact in the possible commercialization of the process, and an academic impact in providing undergraduate engineering students with exposure to a quickly growing part of the chemical industry.

### *Current Industrial Reactions*

Processes have been in existence for years to produce aromatic thiols. These methods generally consist of reduction or thiolation reactions.[5] These reactions have references that go back to the 1920's and 30's when the processes were developed at the laboratory

scale. The particular case focused on herein is the reduction of aromatic sulfonyl chloride to the corresponding aromatic thiol. There are several methods by which aromatic thiols can be produced.

At first, aryl diazonium chlorides were treated with potassium ethyl xanthogenate and heated in the presence of alkalis to form aryl thiols.[6] This process had several undesirable qualities that made it unsuitable for industrial scale-up from the laboratory. It had many side reactions that reduced the overall yield of product and if conditions were not monitored and maintained, then occasional violent explosions could occur. A more promising method for industrial production was found in the reactions that are still used widely today. The original process used the reaction illustrated in Figure 2-1.[6] Modern advancements and industrial research on the actual reaction has changed the reaction, which is reported by DuPont and shown in Figure 2-2.[2]

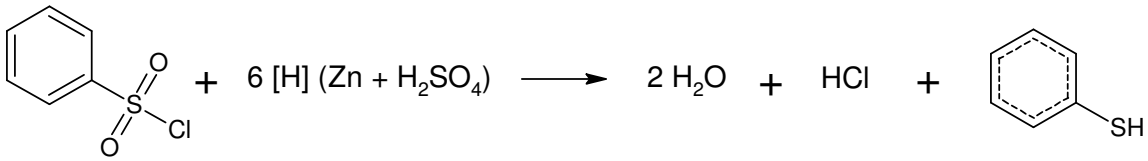


**Figure 2-1.** Production of thiophenol by Zn reduction. The reaction is carried out in dilute acid on the laboratory scale, ca. 1940.

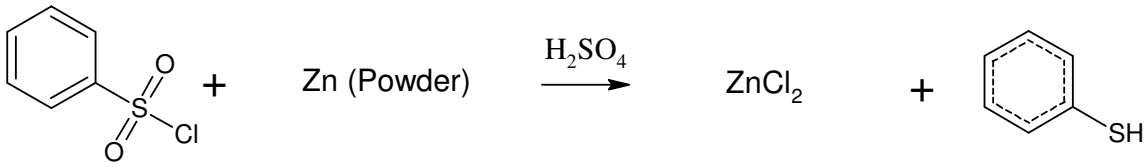


**Figure 2-2.** Current industrial standard reaction for production of thiophenol. Stoichiometry is incorrect, but figure was taken directly from reference.[2]

Zinc powder, as shown in the above reactions, is frequently used as the reducing agent in the presence of a dilute acid.[7] This method results in a by-product of, zinc chloride ($ZnCl_2$), which must be separated from the thiol and disposed of properly.[8] The specific hazards of zinc and zinc chloride to the health and well-being of humans, animals and the environment are well documented and the effects are quite broad. Though less pervasive and less dangerous than other metal-based environmental poisons like arsenic, lead, mercury and cadmium, zinc levels are still cause for concern and investigation in cases of waste disposal, site clean-up and possible groundwater contamination.

Worldwide, governments have restrictions on the amount of zinc that can be found at sites and in groundwater or wastewater flows. References on zinc based investigations and studies on everything from remediation of military sites[9] to veterinary impact of mine tailings on grazing lands[10] are easily located. Current specifications for waste disposal of zinc stand at less than one (1) part per billion zinc. Hence, waste disposal from this process for producing aromatic thiols becomes problematic and expensive.[2]

Yet, production of aromatic thiol compounds is a necessary part of our economy's infrastructure.

Even though zinc is one of our essential elements of life, as with any metal there is a possibility of overdosing or poisoning. At high levels, zinc is known to cause toxic effects on various tissues and organs including the hematopoietic system, cytogenetics, biochemistry and endocrine system function.[11] With the recent increase of zinc's use as a food additive or as part of a self-medicating, anti-fungal regimen any intake of zinc from environmental sources is more likely to make a physiological impact. In addition, zinc chloride specifically has usefulness as a smoke-screen agent with military and civilian applications. However, as evidence of the substance's toxicity becomes more prevalent, its use has been curtailed. The use of zinc chloride screen agents in enclosed structures and confined spaces is now banned by the U. S. military after a study on the long term effect of an accidental, short-term (5-10 minutes) exposure during a training exercise when the participants were without protective breathing apparatus.[12] The soldiers showed a decrease in lung diffusion capacity and overall lung capacity of 16% and 4%, respectively, and elevated levels of zinc in their blood persisted for four weeks after the modest exposure. Though the symptoms began to normalize after 6 months of follow ups, the potential damage of zinc chloride exposure is proven. These are the chemical, health and environmental impacts that industrial aromatic thiol producers are paying for in their waste disposal and remediation expenses.

*Novel Thiol Technology*

In the interest of a cleaner Earth and by using the tenets of Green Chemistry,[1] the zinc-acid process, which produces by-products that damage the environment, the population and the ecosystem, a new system for converting aromatic sulfonyl chlorides to aromatic thiols was developed using palladium on carbon (Pd/C) catalysts for hydrogenation of the aromatic sulfonyl chlorides.[2] The only by-products were water and hydrochloric acid, which could be recycled into other processes or sold as industrial products. Hence, the production of the zinc chloride and the use of zinc powder as a reducing agent with their environmental consequences are eliminated. The work from DuPont focused on the conversion of 2, 5-dimethylbenzene sulfonyl chloride to 2, 5-dimethylthiophenol as shown in Figure 2-3.

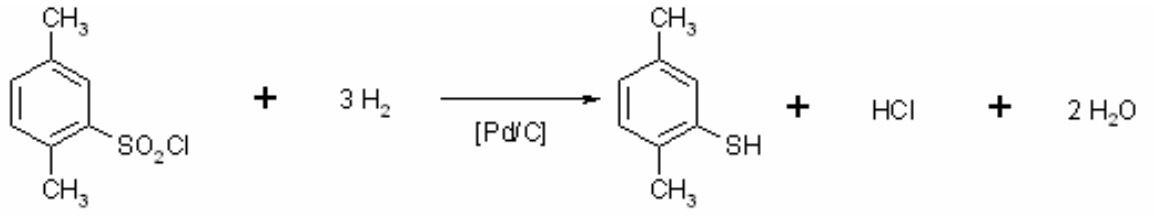


**Figure 2-3**. The overall sulfonyl chloride to thiol reaction.

Preliminary work by DuPont indicated the overall conversion of the aromatic sulfonyl chloride could be represented by first order kinetics.[2] However, kinetics were not proposed for the secondary reactions. Figure 2-4 illustrates a probable stoichiometric

reaction sequence that occurs on the path to production of an aromatic thiol. The interaction of the reactants, intermediates and products with the Pd surface is not illustrated. The proposed first order kinetics for the conversion of an aromatic sulfonyl chloride suggests that either the adsorption of the sulfonyl chloride or the initial consumption of adsorbed sulfonyl chloride is the rate controlling step.

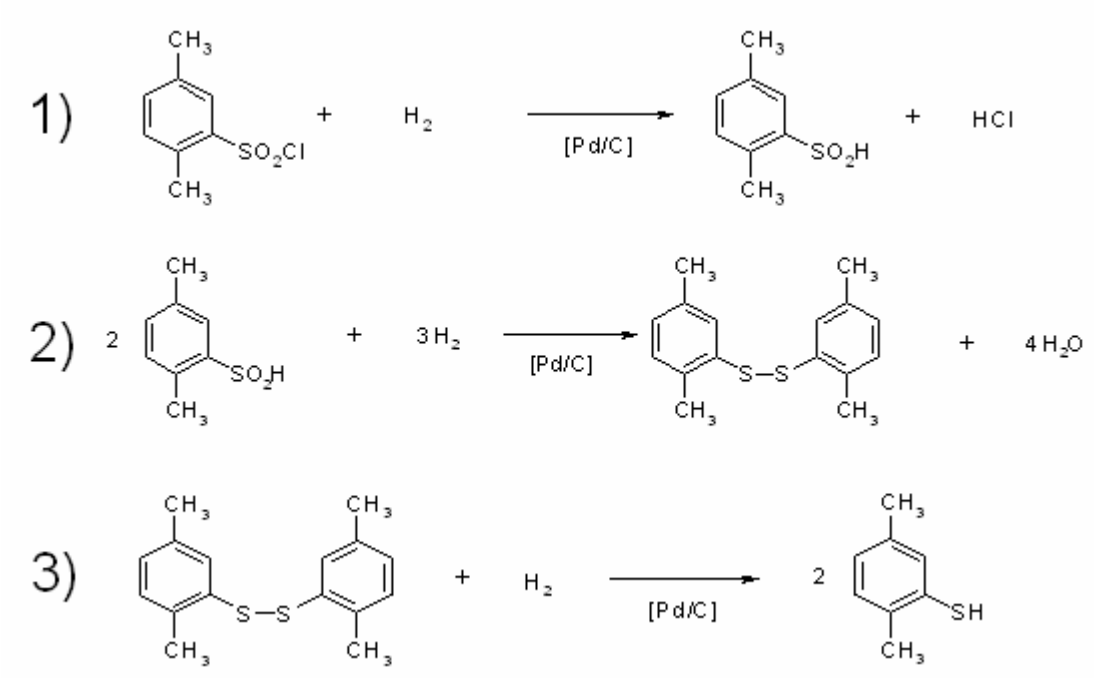


**Figure 2-4.** The steps of the overall reaction. No side reactions are shown.

The advantages of this process over the current industrial standard for thiol production are obvious. Unit operations utilized in each process are very similar. Reactor and transporting vessels for the current process must be acid resistant as they must be in the

novel process. Pd/C catalyst and Zn powder handling are very similar with the exception of particle sizes being larger for Pd/C and thus filter/recovery processes become easier. Most importantly, in the novel process zinc powder waste disposal and production of zinc chloride are avoided. With the ease of recovery of the Pd/C catalyst, waste disposal and remediation costs are greatly reduced, and DuPont's initial data shows that production yields are increased as well.

## 2.2 - Quantum Mechanics

*The Roots of Quantum Theory*

The field of quantum mechanics arose from a discovery in 1900 by Max Planck. He determined he could accurately describe blackbody radiation at all temperatures if he made the assumption that the body could not radiate energy continuously but only in small packets or quanti.[13] While most of his contemporaries scoffed at the notion and believed that a future derivation would not need to utilize the quanti, one of them didn't. Albert Einstein used the quantum hypothesis to explain another problem plaguing physicists at the time, the photoelectric effect. In 1900 there wasn't a lot of data generated on these subjects and the methods of measurement weren't nearly as accurate as today's, but by the 1920's the theory was widely accepted and it had lead to numerous advances in all areas of physics. Simply put, classical physics was not equipped to handle the questions that physicists were asking and the quantum theories were. There is a limit to their usefulness though. Quantum suppositions and calculations are only needed when working on the order of atomic dimensions. If the action or angular

momentum involved in a physical event is orders of magnitude greater than Planck's constant ($h$ = 6.626 x$10^{-27}$ erg-sec), classical mechanics will describe the event with satisfactory accuracy.[13] The angular momentum of a balance wheel in a watch is about $10^{24}h$. The energy of accelerating an electron to the screen of a television tube is $10^{10}h$. In these events the quantization of the action is irrelevant because it is undetectably small when compared with the overall event.[13] The angular momentum of electrons about a nucleus, rotations of gaseous molecules and emission of radiation from atoms are at most a few times Planck's constant and thus to be properly described the quantization of their action and angular momentum must be taken into effect.

The basics of modern quantum mechanics are defined by Schrödinger's equation, which is an eigenvalue equation.

$$H\Psi = -\frac{h}{i}\frac{\partial \Psi}{\partial t}$$

Where:

H = the Hermitian operator called the Hamiltonian,

$h$ = Planck's constant,

t = time,

i = the imaginary number,

and $\Psi$ = the state function.

The next equation shows the substituted classical Hamiltonian for a particle moving through a conservative force field or potential, which is defined in the paragraph below.

$$\left[\frac{h^2}{2m}\nabla^2 + V(r,t)\right]\Psi(r,t) = -\frac{h}{i}\frac{\partial\Psi(r,t)}{\partial t}$$

Where:

r = position (a vector),

m = mass of particle,

and V = potential function.

This equation is frequently seen in Cartesian coordinates, as shown below:

$$\frac{h}{2m}\left(\frac{\partial^2}{\partial x^2} + \frac{\partial^2}{\partial y^2} + \frac{\partial^2}{\partial z^2}\right)\Psi(r,t) - V(r,t)\Psi(r,t) = \frac{h}{i}\frac{\partial}{\partial t}\Psi(r,t)$$

Where:

All variables are the same as in the first equation,

and x, y and z = Cartesian spatial coordinates.

This equation forms the basis of how a particle moves through a conservative potential function. The definition of a conservative potential function is one in which a change in potential between arbitrary points A and B is not dependent upon pathway. The question is how is this basic equation utilized by modern techniques?

*Quantum Chemistry*

Finding and describing approximate solutions to the electronic Schrödinger equation has been a major preoccupation of quantum physicists since the birth of quantum

mechanics.[13] The electronic Schrödinger equation begins with the non-relativistic, time-independent form of the equation and utilizes the Born-Oppenheimer approximation, a pillar of quantum chemistry. A more detailed qualitative discussion of the approximation can be found in the text by Szabo and Ostlund,[14] while the quantitative aspects are discussed in a different publication by Sutcliffe.[15] The Born-Oppenheimer approximation states that since nuclei are much heavier than electrons, they move more slowly. Thus, electrons can be considered to be moving around a fixed field of nuclei and the nuclei-nuclei repulsion effects can be considered to be a constant. The eigenfunction solutions to the electronic Schrödinger equation are known as the electronic wave functions. They describe the motions of electrons and depend explicitly on the nuclear and electronic coordinates, but do not explicitly contain the nuclear motion. It is this electronic solution which quantum chemists seek. Further, upon finding an electronic solution, the researcher can go back and use the Born-Oppenheimer approximation to average over the electronic energies and determine a nuclear solution to the Schrödinger equation. This solution returns the values for the total energy along with the vibrational, rotational and translational components of that energy. However, these calculations, called frequency calculations in the Gaussian03[16] software package, have to be analyzed carefully unless a stationary point has been initially established.

*Hartree-Fock and Molecular Orbitals*

At this point in the description, the nuclei have been fixed and the electrons are free to move about amongst them. This motion must be better quantified if it is to be used for

any useful calculations. When a chemist thinks of an atom, most of them picture a heavy, positively charged center with a cloud of electrons about the nucleus. This is the picture they were taught in their basic chemistry classes. These are the structures they drew to learn about how atoms interact to make molecules. This is the simplest way to mentally picture the Hartree-Fock approximation.

The Hartree-Fock approximation uses molecular orbital approximation. Deeper than that, by quantifying the orbitals predicted in the approximation, it is possible to mathematically define the way that the electrons are moving within the fixed nuclei field from above. The idea of basis sets arises from this aspect of the Hartree-Fock approximation.

Basis sets are the way that quantum chemists define molecular orbitals mathematically so that they can be solved. Basis sets consist of atomic orbitals and there are two types, Slater-type orbitals and Gaussian-type orbitals. There are two main considerations in the choice of a basis. The first is that one desires to use the most efficient and accurate functions possible, thus using the fewest possible terms for an accurate representation of the molecular orbitals.[14] On that point, Slater functions are best. They decay exponentially with distance from the nuclei.[17] The second consideration is the speed of the many, individual two-electron integral evaluations that must be performed at every step in the calculation. Gaussian functions are 4-5 orders of magnitude faster than Slater functions due to the Gaussian Product Theorem.[18] The formulation of Gaussian Type

Orbitals allows for an analytical solution for the many 2-electron interactions that must be performed during a calculation, while Slater Type Orbital solutions to electron-electron interaction remain numerical. So, from a calculation speed point of view, Gaussian functions are the obvious choice.

Since they are so much easier to use computationally, the most common practice is to take "primitive" Gaussian orbitals and create a basis set using "contracted" Gaussian orbitals. Contracted Gaussian orbitals are simple, linear combinations of primitive Gaussian orbitals. The increase in the workload of using contracted Gaussian orbitals to approximate orbital functions (of whatever type) is still far less than actually calculating the Slater orbital functions.[14] The contracted Gaussian orbitals are the building blocks of the applied basis sets used in this work.

*Basis Sets*

Basis sets are named by their functionality. The minimum basis set STO-3G is a specific member of the bigger STO-LG family. They are named because the contracted Gaussian orbitals consist of L primitive Gaussians and they are set up with parameters to approximate Slater-type orbitals of the type s and p. STO-3G uses three primitive Gaussians to construct a contracted Gaussian to use to approximate Slater functions. STO-3G is widely known as the minimal basis set for quantum chemical calculations. The first step up from minimal basis sets are double-zeta basis sets. They simply use two basis functions in the place of each minimal basis function. Triple-zeta and quadruple-

zeta basis sets are also used, but computation time quickly becomes a limiting factor in evaluating real molecular systems with these expansive basis sets.

An example of a hybrid basis set is the split valence basis sets that are easily identified by their X-YZG monikers. X, Y and Z are integers that refer to the numbers of primitive Gaussians to represent the s- and p-type orbitals of elements. X is the number of primitive Gaussians used to represent the inner shell (non-valence) orbitals while Y and Z are the double zeta representation of the valence shell electrons. These split valence approaches are common because they save on computation time and simulate reality in the fact that non-valence shell electrons contribute little to most chemical properties. 6-31G is a common split valence basis set. It contracts 6 primitive Gaussians for the inner shell electrons and uses a contraction of 3 primitive Gaussians (inner) and 1 primitive Gaussian (outer) to represent the valence shell. The addition of the split valence shell allows more flexibility in the calculation and simulation of the valence electrons and their orbits about the nucleus. This leads directly to more accurate simulations for very little increase in computation time.

In addition to using split valence basis sets, in the case of heavy atoms ($3^{rd}$ row and above) it is sometimes useful to lump the inner shell electrons in with the already frozen nuclei. The methods that handle this are called Effective Core Potentials (ECP) and they turn the inner shell (non-valence) electrons into simple potentials since they have so little effect on the chemical properties of the atom. One of the most widely used versions of

ECP, the Los Alamos National Labs 2 Double Zeta ECP (LANL2DZ), is effective in the work shown in this paper for atoms of sulfur, chlorine and palladium. The benefits are found in greatly reduced computation time since many of the inner shell electrons of these larger atoms are thrown in with the ECP and don't have to be individually calculated. However, some accuracy is lost in this approach as every electron that is active in the molecule is not simulated specifically. It is just another example of the assumptions individual researchers may choose to make in the course of a quantum mechanical investigation.

Sometimes, split valence basis sets fall short of predicting actual atomic behavior and further functions are needed called polarization functions. The basis sets utilizing these functions are known as polarized basis sets and, for Pople style basis sets, are denoted with either one asterisk or two as in, 6-31G* or 6-31G**. These asterisks mean that extra functions are being used to represent the higher angular momentum orbitals for certain elements. The first asterisk means that an additional set of uncontracted d-type orbitals is being added for elements with only s- and p-type occupied orbitals. While, the second asterisk means that p-type orbitals have been added for all hydrogen atoms. As a result these basis sets are sometimes also referred to as 6-31G(d) and 6-31G(d,p) respectively. These basis sets yield results far superior to STO-3G and 4-31G basis sets, but still fall short in some calculations. Larger basis sets can alleviate these shortcomings. The methods include the aforementioned triple and quadruple zeta methods, adding more

polarization functions (d', a double zeta d-type polarization function or perhaps seven f-type orbitals for heavier atoms) and better defining the inner shell electrons.[14]

*Density Functional Theory*

A second approach other than Hartree-Fock (HF) methods has been gaining momentum and widespread use in the last few years, Density Functional Theory (DFT). DFT gets significantly better computational results for only a small increase in simulation time. DFT methods calculate electron correlations utilizing functionals. A functional is defined mathematically as a function of a function. In DFT, the functionals are functions of the electron density which is itself a function of the real space coordinates. DFT uses the functionals to separate the electronic energy into components, each of which is calculated separately. They are the kinetic energy, the electron-nuclear interaction, the Coulomb repulsion and an exchange-correlation term that accounts for the remainder of the electron-electron interaction.

In some DFT methods, the exchange-correlation term is separated into exchange and correlation functionals. Many functionals have been defined, each separate in the way it treats the exchange and correlation components of the calculation. Local exchange and correlations functionals utilize only the electron spin densities while gradient-corrected methods use the spin densities and their gradients in the formulation. Popular gradient-corrected exchange and correlation functions have been proposed by Becke[19] (B) and Lee, Yang and Parr[20] (LYP).

*Hybrid Methods*

Given a basis set and an approach (HF or DFT) the actual calculations performed are very similar. HF simulations make use of the idea of a self-consistent field (SCF). In a SCF a molecule and a basis set are specified first. Then, calculations to obtain an initial guess at the electron density matrix are made. The HF method calculations are performed on that density matrix and at the end a new matrix is generated. The old and new density matrices are compared and if they are consistent to within a degree of convergence (usually set by the user) then the problem is considered solved. If they are not consistent then the process begins again with the new matrix.

DFT methods lack a good exchange energy prediction. HF methods include an exact exchange term as part of its formulation and Becke has incorporated that fact into his own hybrid functionals to a great degree of success. His three parameter hybrid exchange-correlation functional (B3LYP, named so because it uses his own exchange functional and Lee, Yang and Parr's correlation functional) is used extensively in the world of quantum chemistry and in the work discussed in this paper. It uses the inclusion of HF exchange within the realm of a DFT calculation to give accurate results at a good rate of speed. Combinations of other exchange functionals and correlation functionals lead to other hybrid methods and there are several of them in use in quantum chemistry research today.

*Quantum Chemistry Research*

Simulations and research in the quantum chemistry field is highly diversified. A large sector of the community is oriented towards understanding protein folding, metal ion effects in body chemistry and a host of other biochemical applications. Adsorption to simulated surfaces with wide ranging adsorbed molecules and surface structures are common investigations. The field is simply too broad to discuss it all. Instead, focus is necessary.

Within the confines of simulating catalyst surfaces suitable for hydrogenation and aromatic molecule adsorption, both subjects involved in the work described herein, there are several active researchers performing a host of simulations. While none of them specifically works with the sulfonyl chloride to thiol system discussed previously, there are very similar systems being researched and, far more prevalently, very similar surfaces are being simulated.

A research group in Italy, led by Barone and Duca has been making interesting headway into simulations and experiments focusing on the adsorbing and subsequent hydrogenation of 2,4-dinitro-toluene with palladium.[21,22,23] Though their simulations were not as aggressive as the ones presented in the results section of this paper, their insights into aromatic adsorption and palladium surface simulation[24,25] were instrumental in getting the work presented herein initiated. Many researchers like Neurock,[26,27] Hirschl[28] and Bertani[29] are doing high level simulations of smaller organic molecules

like ethylene and formaldehyde over small palladium and platinum clusters. Another group from Switzerland[30,31] provides a great example of the power of switching between small cluster simulations of surfaces, the method used in this work, and bulk surface simulations of surfaces in their simulations of the adsorption of ketones and quinonyl compounds to platinum catalytic surfaces. Work by Efremenko[32,33,34,35] and Ishiwatari[36] show the advantages and pitfalls to working with extremely small clusters of metal atoms and using them to represent surfaces. The works cited above are a basis for everything that is presented in the results section of this publication. Their insights and observations into quantum mechanical simulation of aromatic systems or Pt/Pd catalyst systems were of great help in getting started.

## 2.3 - Economics Review

*Economics in the Specialty/Fine Chemical Industry*

A brief look at the state of the global specialty chemicals economy follows. Through the first 2 quarters of 2007 growth in the chemical industry was steady. Productions levels were on the rise across the globe.[37] Trends are heading towards consolidation of chemical distributors and this is making chemical purchasers a little nervous.[38] No one in business likes to see their choices narrow. It's a rule of economics, fewer suppliers because of consolidation reduces competition and can force up prices. The consolidation is happening at the top of the Purchasing's Top 100 list too as there was a bidding war for the rights to acquire the 4$^{th}$ largest chemical distributor between the 3$^{rd}$ largest and the overall biggest chemical distributors in the world in the spring of 2007.[38]

North American production activity grew but only slightly in the first part of 2007 due partly to a decline in agrochemical production. Western European production increased as well, while the Asia/Pacific region continued their recent booming trend. Overall production in the Asian markets jumped nearly 4% from December 2005 to December 2006. Strongest gains were seen from India, Malaysia and Thailand.[37] Gains in the Chinese markets can still be found, but competition has become fiercer since WTO accession and a diversified market has developed there. The Chinese chemical market is especially hard to predict with the co-existence of large state-owned enterprises, multi-national chemical companies and private enterprises.[39] Specialty chemical producers are still flocking there to open new ventures because of the relatively cheap but skilled workforce and, in some cases, more lax environmental concerns.

Specialty chemical makers are pouring dollars into their R&D efforts, seeking to improve project success, speed up commercialization and simply generate higher returns. They are focusing on finding the next technology that will add to their bottom line. To do this they are focusing their R&D budgets, targeting fewer projects that have a better chance of returning their investment and adapting strategies to acquire startup companies with truly unique technologies.[40]

Closer to home for the work done in this project, the intermediates market is still going strong, on target with the rest of the specialty chemicals industry. Aromatic thiols

themselves are in demand and the most popular of them, benzenethiol, is being produced at a level of 10 million lb/yr.[2] The aromatic thiol price has recently gone through a decline as producers from Asian markets exercise their ability to make a quality product for less money than their competitors. The price in summer of 2007 stood at $2.27/lb benzenethiol.[41] In fact, a rough internet search for distributors of benzenethiol in bulk only turned up Asia/Pacific based chemical manufacturers.

# 3. SURFACE SIMULATION AND ADSORPTION CALCULATIONS

## 3.1 - Introduction

Aromatic thiols are of industrial importance due to their use in the manufacture of agrochemicals, polymers, pigments, dyes and pharmaceuticals.[3,4] Processes have been in existence for years to produce aromatic thiols. These methods generally consist of reduction or thiolation reactions.[5] The particular case focused on here was the reduction of aromatic sulfonyl chloride to the corresponding aromatic thiol. Zinc has been frequently used as the reducing agent in the presence of a dilute acid.[7] This method, developed in the early 20$^{th}$ century, results in a by-product of zinc chloride, which must be separated from the thiol and properly disposed of.[8] The specific hazards of zinc chloride to the health and well-being of humans, animals and the environment are well documented and the effects are quite broad.[9,10,11,12,42]

In the interest of a cleaner Earth and by using the tenets of Green Chemistry,[1] the zinc-acid process, which produces by-products that damage the environment and the ecosystem, was improved upon. A new system for converting aromatic sulfonyl chlorides to aromatic thiols was developed using palladium on carbon (Pd/C) catalysts for hydrogenation of the aromatic sulfonyl chloride.[2] The only by-products were water and hydrochloric acid, which could be recycled into other processes or sold as industrial products. Hence, the production of the zinc chloride with its environmental

consequences is eliminated. This work focuses on the conversion of 2, 5-dimethylbenzene sulfonyl chloride to 2, 5-dimethylbenzenethiol as shown in Figure 3-1.

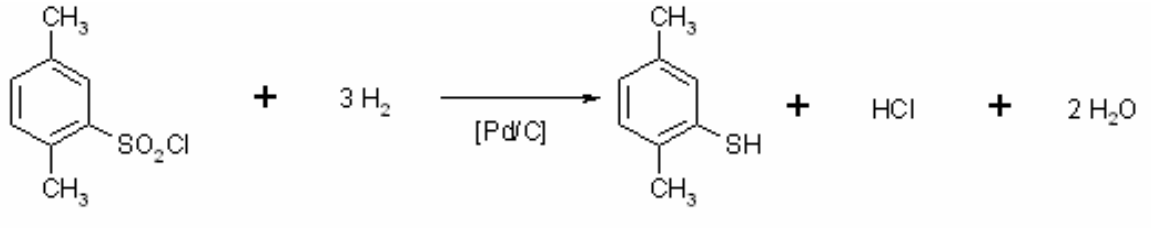


**Figure 3-1**. The overall sulfonyl chloride to thiol reaction.

Preliminary work by DuPont indicated the overall conversion of the aromatic sulfonyl chloride could be represented by first order kinetics.[2] However, kinetics were not proposed for the underlying reactions. Figure 3-2 illustrates a probable stoichiometric reaction sequence that occurs on the path to production of an aromatic thiol. The interaction of the reactants, intermediates and products with the Pd surface is not illustrated. The proposed first order kinetics for the conversion of the aromatic sulfonyl chloride suggests that the adsorption of the sulfonyl chloride in Figure 3-2 is the rate controlling step. By utilizing quantum mechanical calculations one might gain insight into the actual reaction mechanism for the conversion of the aromatic sulfonyl chloride to the thiol. This section focuses on the adsorption steps by utilizing density functional theory and three different (100) Pd surfaces.

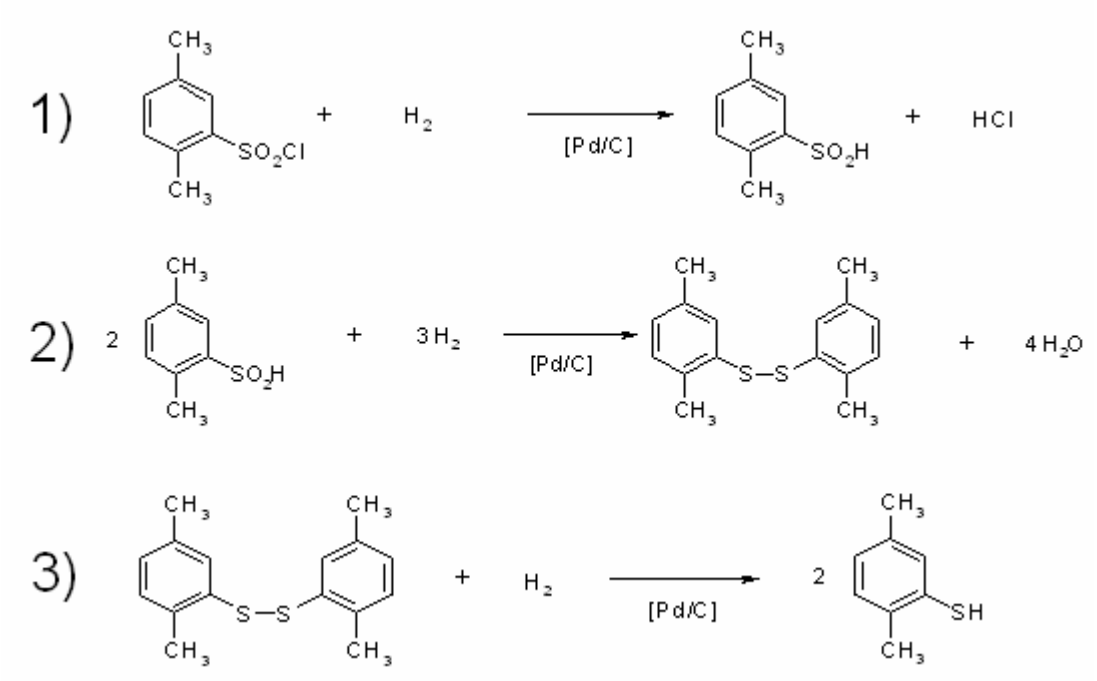


**Figure 3-2.** The steps of the overall reaction. No side product reactions are shown.

### 3.2 - Computational Methods

All calculations were performed on a 64 node (128 processor) cluster. Each node was an Apple G5 Xserves with dual 2.0 GHz G5 processors which have 2GB RAM, an 80GB hard drive, and a gigabit ethernet. The head node was of the same type but utilizes the expanded capacity of 4GB RAM, 750GB internal HD and 2.5TB of RAID storage with a fiber channel for user files. All nodes were interconnected with wire speed foundry gigabit switches. This node cluster is the exclusive property of the College Of Engineering at Texas A&M University.

These investigations utilized the Gaussian03[16] software package with LINDA. Density functional theory (DFT) was used for all calculations at the Becke-3 exchange and Lee-Yang-Parr correlation (B3LYP) level.[19,20] H, C, and O atoms utilized the 6-31G(d') basis set while the S, Cl and Pd atoms used the Los Alamos National Labs 2-double-zeta basis set (LANL2DZ).[43] S and Cl molecules were supplemented with one d function each. The LANL2DZ basis set utilized an effective core potential (ECP) which eased the computational load and included relativistic corrections that were especially important for heavy atoms such as Pd. All molecules had a neutral overall charge and were run as restricted with the exception of the proposed thiol anion species which had a total charge of -1.

The proposed simulation process for adsorption progressed as follows. First, the species, was structurally minimized. Then adsorption of that minimized structure on a cluster of palladium atoms which represents the catalyst was simulated. The result of this minimization represented an adsorbed molecule on the catalyst surface.

### 3.3 - Palladium Catalyst Simulation

The first step in the project before the calculations could be run was the question of simulating the catalyst surface. There are two approaches to use for this case. A stand-alone cluster for surface simulation is one case. Generally these clusters are large, flat, contain many molecules and they make for highly accurate simulations. However, they

are computationally bulky. The other possibility is using a small cluster to represent a larger bulk surface. In this second case, no matter the size of the cluster it can be thought of as a small piece of a much larger bulk surface. It is a single representative for simulation that in reality, outside of the formulation within the simulation, is surrounded by exact duplicates of itself creating the catalyst surface. That vision of the simulated cluster allows for more flexibility within the calculations. This second method is used herein and the idea of the simulated cluster being surrounded by other duplicates to represent the catalyst surface is crucial in some of the decisions made about the adsorption calculations.

In testing a Pd-based reaction system for the effects of particle size and charge distribution throughout the catalyst surface, Duca and Barone simulated adsorption of various amino-nitro-benzene molecules over a layer of six Pd (100) molecules.[21] Their work also showed a scheme for simulating a three-layered Pd matrix with only 22 atoms.[24] Ishiwatari and Tachikawa showed good planar representations of metal catalyst molecules calculated with the same theoretical level and basis sets that are used in this study.[36] An idea for a cluster with fixed bond lengths can be deduced from these works.[24,,32,34,35,44] Various authors varied Pd-Pd distances from 0.275 nanometers down to 0.2372 nanometers. A median distance of 0.25 nm between the two extremes was utilized in Efremenko and Sheintuch's work for optimizing small palladium structures in square (rectangular) planes[35] and that distance was used in the work described below.

A good model cluster should be symmetrical to reduce the possible reaction sites that must be investigated, have multiple layers, have as few metal atoms as possible and still give a reasonable representation of bulk Pd. A set of palladium clusters were developed, herein, that ranged from the complicated, which encompass many of the qualities of a good cluster, to the simple, which were more computationally feasible.

Three different clusters were designed, as shown in Figure 3-3. They are each based on a (100) crystal and have 6, 8, and 13 Pd atoms. The clusters were named for the number of palladium atoms included in the model; $Pd_6$, $Pd_8$, and $Pd_{13}$, respectively. All metal atoms were locked into place during all calculations. Freezing of the palladium atom coordinates was necessary for two reasons, accurate depiction of the restricted environment of the crystalline structure of the catalyst in the reactor and also decreasing the computational load in running the simulations.

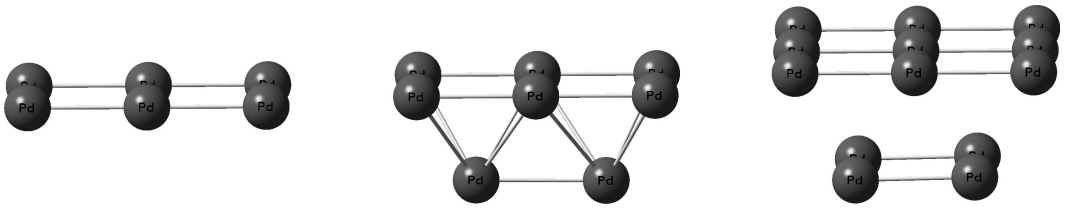


**Figure 3-3** – A diagram of each of the three palladium structures. Each are described briefly below. $Pd_6$ – a single layered six atom structure. $Pd_8$ – a two layered, 8 atom structure in a (100) structure 6 atoms over 2 atoms. $Pd_{13}$ – a two layered, 13 atom structure in a (100) structure, 9 atoms over 4 atoms, equivalent to two $Pd_8$s side by side.

## 3.4 - Adsorption of Aromatic Sulfonyl Chloride

*Minimizing the Reactant Structure*

Initially, a geometry optimization of the reactant molecule was performed. This minimization provided the minimum energy configuration for the molecule that would be adsorbed onto the proposed palladium clusters. The previous holders[2] of the technology determined that the reaction rates were well approximated by a first order curve in the reactant. The result of the geometry optimization is presented in Figure 3-4. Frequency calculations showed no imaginary modes. The crystal structure of the reactant

has not been determined, but similar compounds have been analyzed by crystallographic methods. Therefore, a comparison of selected bond lengths and bonding angles from the simulations and experimental data on 4-nitro and 2-nitro benzene sulfonyl chloride are presented in Table 3-1.[45,46] Haist [47] investigated 2,4-dinitro benzene sulfonyl chloride including experimental and computational methods showing that, in general, the computational results differed from experimental values by up to 0.091 Å (avg. 0.027 Å) on bond lengths and by up to 2.4 degrees (avg. 1.41 degrees) on angles. The comparisons shown in Table 3-1 varied in bond lengths by up to 0.125 Å (avg. 0.045 Å) and in angles by up to 3.17 degrees (avg. 1.45 degrees). These bond length values decreased to 0.049 Å (avg. 0.03 Å) if consideration of the sulfur-chlorine bond was ignored. This bond could have been greatly affected by the presence of two additional, negatively charged oxygen atoms in each nitro- group containing molecule. The above values showed that the simulated structures were within the norm when compared to similar computations and similar molecules. Figure 3-5 shows the charge distribution for 2,5-dimethylbenzene sulfonyl chloride.

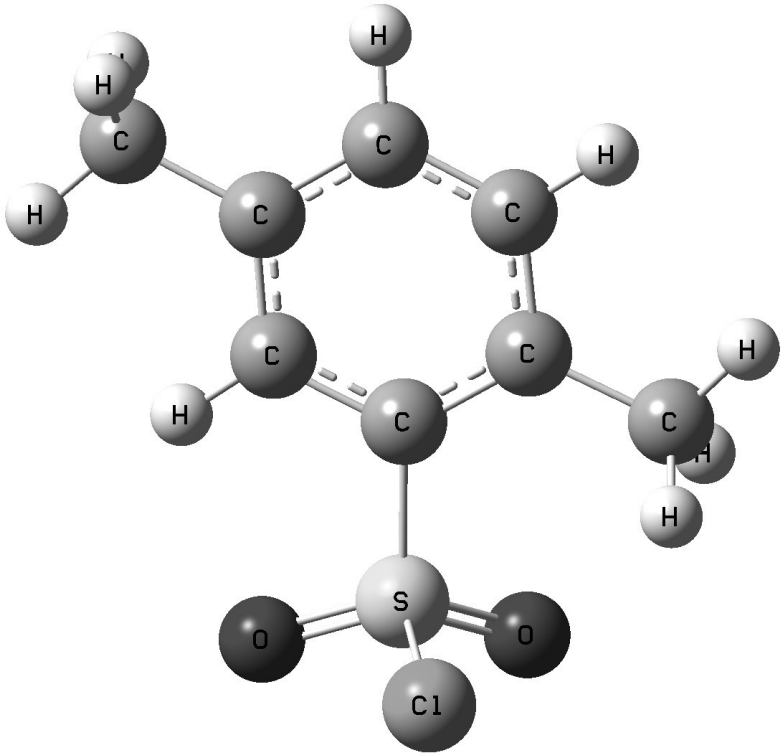


**Figure 3-4.** The minimized structure of 2,5-dimethylbenzene sulfonyl chloride. Dipole moment 5.551 Debye, C-S bond is 1.797 Å, S-O bonds are 1.467 Å, and S-Cl distance is 2.145 Å.

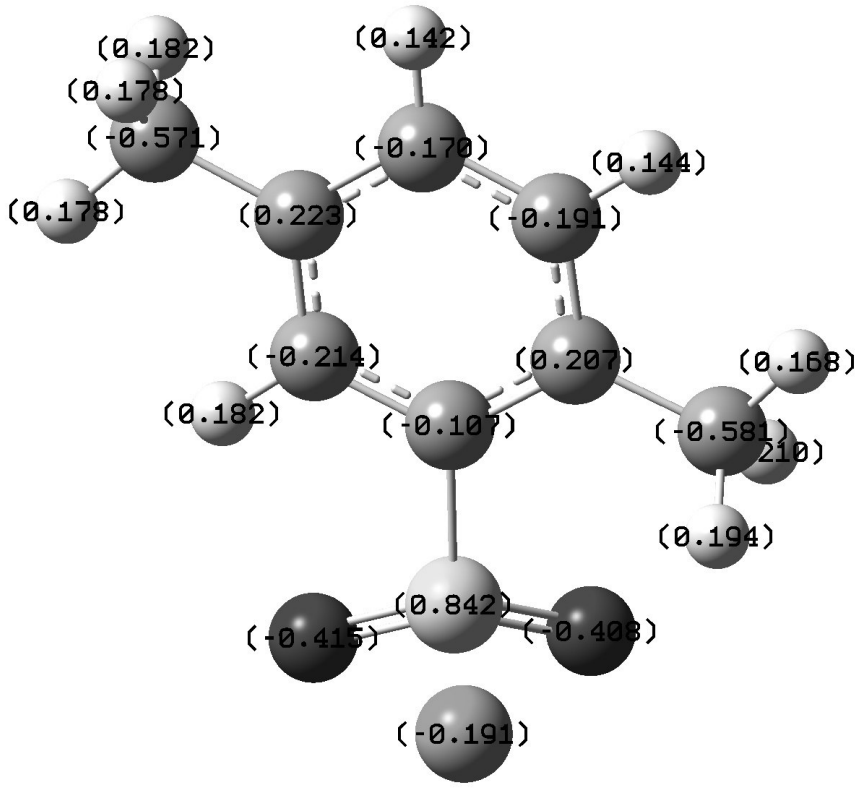


**Figure 3-5.** The minimized structure of the reactant molecule showing the charge distribution. Notice that the sulfur atom has a large positive charge (0.842), the oxygen atoms have strong negative charges (-0.415, -0.408) and the chlorine is slightly negative (-0.191). The S-Cl bond shown in Figure 3-4 is sometimes omitted when the software renders these graphics.

**Table 3-1.** Selected bond angles and bond lengths from experiments or computations done on the structures of molecules of X-benzene sulfonyl chloride. The first three columns are x-ray data from crystal structures of the compounds listed.[45,46] The fourth column contains the computational results from this study done at the B3LYP/6-31G(d') level. Bond lengths are reported in Å. Angles are reported in degrees.

| Compound | X = | 2-Nitro | 2-Nitro | 4-Nitro | 2,5 Dimethyl |
|---|---|---|---|---|---|
| **Bonds** | **S-Cl** | 2.034 | 2.029 | 2.019 | 2.145 |
| | **S-O1** | 1.428 | 1.423 | 1.418 | 1.467 |
| | **S-O2** | 1.425 | 1.426 | 1.421 | 1.467 |
| | **S-C1** | 1.765 | 1.762 | 1.76 | 1.797 |
| | **C1-C2** | 1.402 | | | 1.402 |
| | **C2-C3** | 1.384 | | | 1.408 |
| | **C3-C4** | 1.407 | | | 1.394 |
| | **C4-C5** | 1.371 | | | 1.401 |
| | **C5-C6** | 1.39 | | | 1.397 |
| | **C6-C1** | 1.408 | | | 1.399 |
| **Angles** | **Cl-S-O1** | 107.7 | 107.35 | 106.63 | 105.63 |
| | **Cl-S-O2** | 107.4 | 106.47 | 106.04 | 105.78 |
| | **Cl-S-C1** | 101.3 | 102.67 | 101.81 | 100.71 |
| | **O1-S-O2** | 118.9 | 120.76 | 120.84 | 121.53 |
| | **O1-S-C1** | 110.4 | 108.44 | 109.77 | 109.72 |
| | **O2-S-C1** | 109.3 | 109.62 | 109.93 | 111.12 |
| | **S1-C1-C2** | 122.2 | 123.68 | 117.72 | 121.65 |
| | **S1-C1-C6** | 117 | 116.75 | 118.3 | 115.13 |

*Adsorption of the Reactant on a (100) Pd Surface*

The experimental reactor would contain the catalyst and the aromatic reactant molecule just like the previous discussion has, but there was one other addition, the hydrogen reactant, which was not present in the current simulations. The adsorption optimizations showed a picture of what the aromatic molecules would be doing on the surface of the catalyst without the presence of hydrogen.

The orientation of the molecule when adsorbed was not known. Several guesses had to be made on the direction of the adsorption. The Barone and Duca articles,[21,22,23,24] showed that there can be several different orientations for adsorption of an aromatic molecule on a palladium surface. Several adsorption modes were evaluated for the $Pd_6$ cluster. $Pd_6$ was the least computationally intense of the clusters and provided insight into the lowest energy adsorption mode. All trial structures began with a 3 Å distance between the nearest carbon or sulfur atom to the surface and several different adsorption modes were used. These modes and their direction of rotation within the calculation are shown in Figure 3-6.

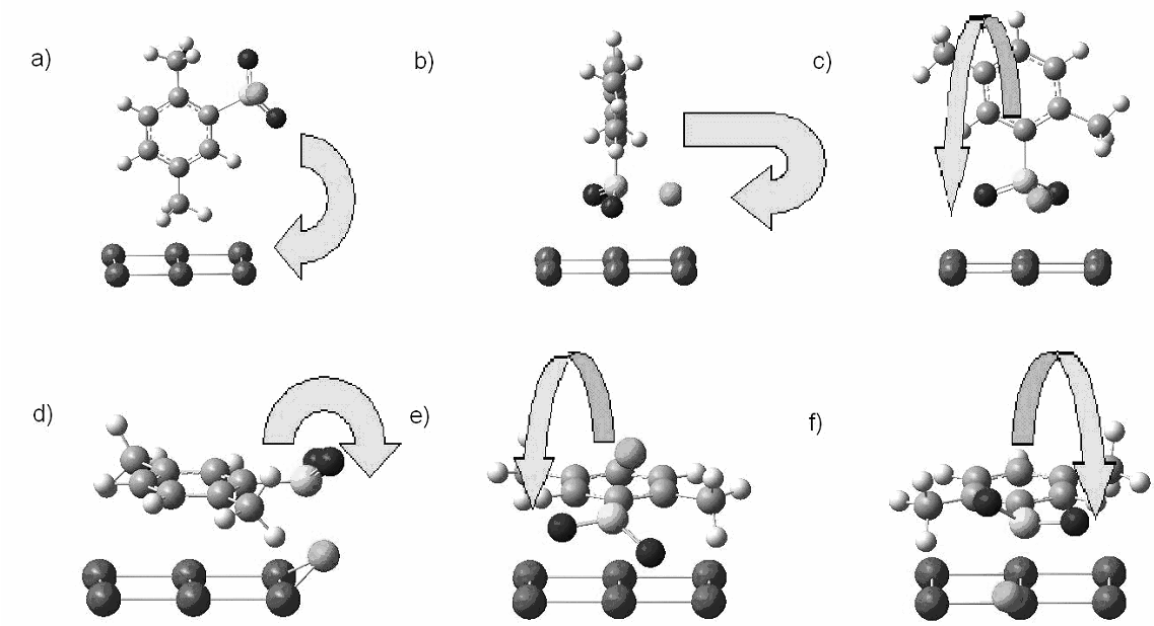


**Figure 3-6.** Initial configurations used for the sulfonyl chloride adsorption calculations. The movements from the first steps of the DFT minimizations are represented by the arrows. In every case, the driving force was the need for one or both of the oxygen atoms to interact directly with one or more of the palladium atoms. a) Adsorption of the molecule via one of the methyl groups in the two orientations possible on the non-symmetrical $Pd_6$ cluster. b) A vertical adsorption mode via the sulfonyl chloride functional group. c) Same as (b) but in the opposite $Pd_6$ orientation. d) A horizontal adsorption mode with the chlorine molecule interacting with the surface immediately. e) A horizontal adsorption that is simply (d) inverted and in the opposite $Pd_6$ orientation. f) A horizontal adsorption that is (d) in the opposite $Pd_6$ orientation or (e) inverted.

All of the different adsorption conformations showed approximately the same behavior. A step by step progression during optimization could be observed from the output files as the calculations proceeded. Each calculation's first step was to back the aromatic molecule away from the palladium cluster, to a distance greater than 3 Å, and then the molecules begin to rotate. Again, these rotations are shown in Figure 3-6. As deduced from the data, the path to the minimum energy was in the direction of having the

sulfonyl chloride portion of the molecule interact directly with the Pd matrix. This particular adsorption configuration was further supported by the literature. [48,49,50,51,52,53]

Sulfur is a well known poison for industrial hydrogenation/dehydrogenation catalysts.[48,49,50,51,52] It binds to palladium, especially in cracking and refining operations, which decreases the reaction area available on the catalyst. The reported binding energies ranged from -110 to -125 kcal/mol.[48,52] Oxygen and chlorine also bond strongly to palladium surfaces, with energies reported in the -25 kcal/mol range for oxygen and in the -77 kcal/mol range for chlorine.[48,53] All of these individual molecules interacting with palladium in one functional group suggests that the molecular shifts seen in the current adsorption calculations were likely.

These calculations were very time intensive and once the trend of sulfonyl chloride adsorption was clear, all other modes were abandoned in favor of focusing on the vertical adsorptions with the sulfonyl chloride group most closely in contact with the metal catalyst. A case could be made that the horizontal adsorption modes were just as important as the modes that were chosen and should be investigated, but since the Pd clusters are representative of much larger palladium surfaces, the horizontal adsorption modes can be dismissed. The individual clusters are representatives of a single block in the Pd surface which consists of many exact copies in the cluster bound together. The horizontal modes of adsorption were taken from the perspective of a cluster of Pd atoms on the Pd surface that was not centered over the area of computational interest. Simply

put, the simulations have taken account of the wrong block of Pd atoms from the surface. Having taken the view that the cluster can be shifted to represent the best block in the overall Pd surface for adsorption calculation, these horizontal adsorption modes were rotating to positions that were equivalent to those already investigated by the vertical adsorption modes.

*Adsorbing the Reactant to the Catalyst*

The vertical orientations were optimized on the more complicated palladium clusters, $Pd_8$ and $Pd_{13}$ as well. The vertical orientation over $Pd_8$ is shown in Figure 3-7. The minimized, adsorbed 2, 5-dimethylbenzene sulfonyl chloride structures on $Pd_6$, $Pd_8$ and $Pd_{13}$ are shown in Figures 3-8a, 3-8b and 3-9. The frequency calculations for these structures produced imaginary modes, which indicate that a local minimum has not been identified. Since the Pd molecules were frozen during the calculations, the imaginary modes were probably from being frozen while not in a minimum energy structure. As evidence of this, an investigation of the specific vibrations showed some movement of the Pd cluster within the molecular vibrations associated with all of the imaginary modes.

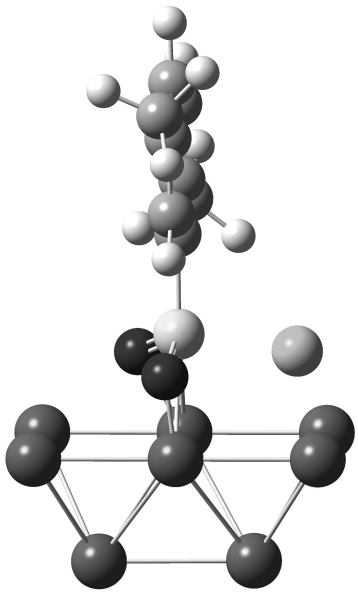

**Figure 3-7.** The starting structure on the vertical adsorption (DFT minimization) calculation. This is a representation of the aromatic sulfonyl chloride molecule over $Pd_8$.

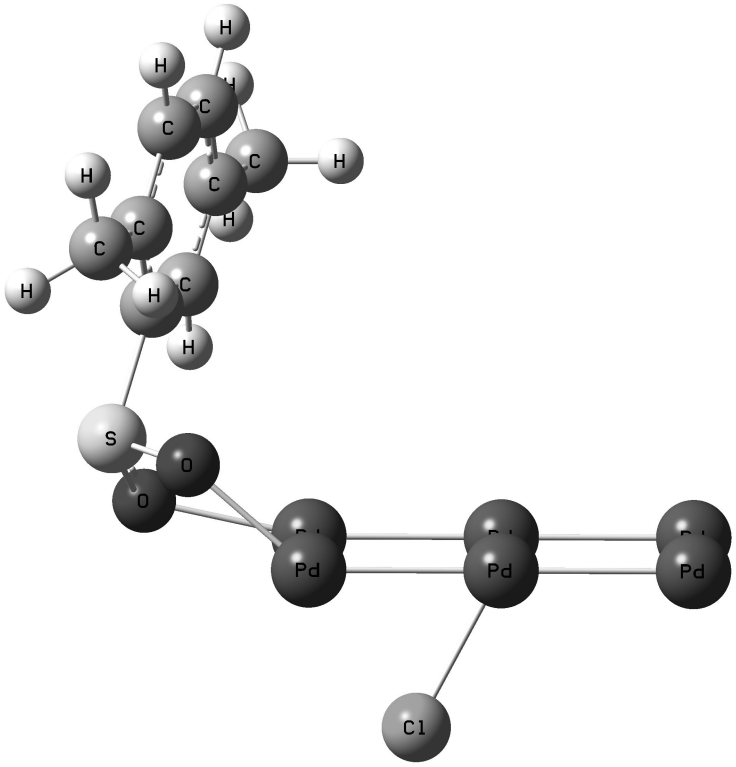


**Figure 3-8a.** The results of the DFT optimization calculations over $Pd_6$. This represents the minimum energy calculated. $\Delta H_{ads}$ = -51.97 kcal/mol.

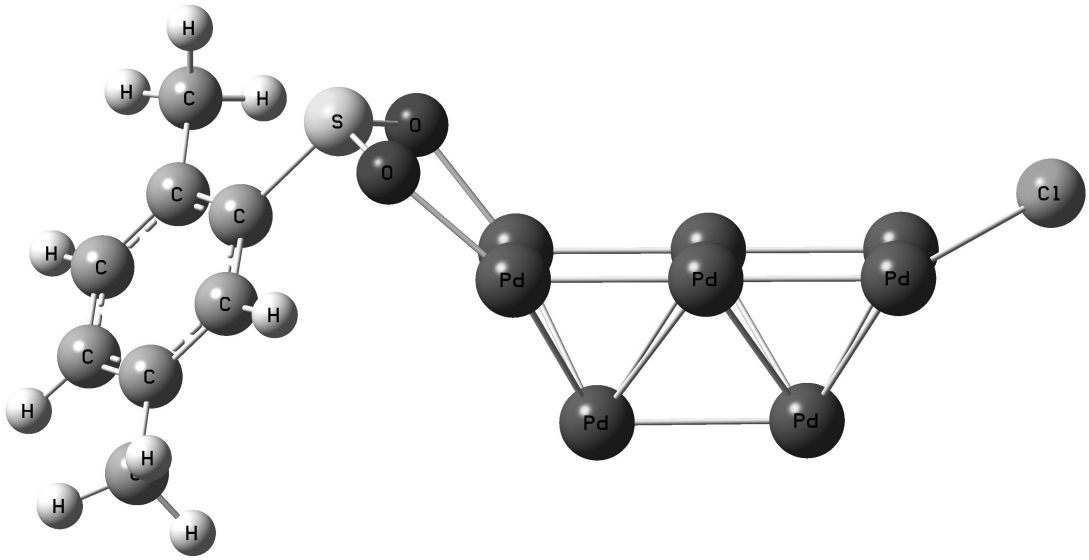


**Figure 3-8b.** The results of the DFT optimization calculations over $Pd_8$. This represents the minimum energy calculated. a) $\Delta H_{ads}$ = -56.28 kcal/mol

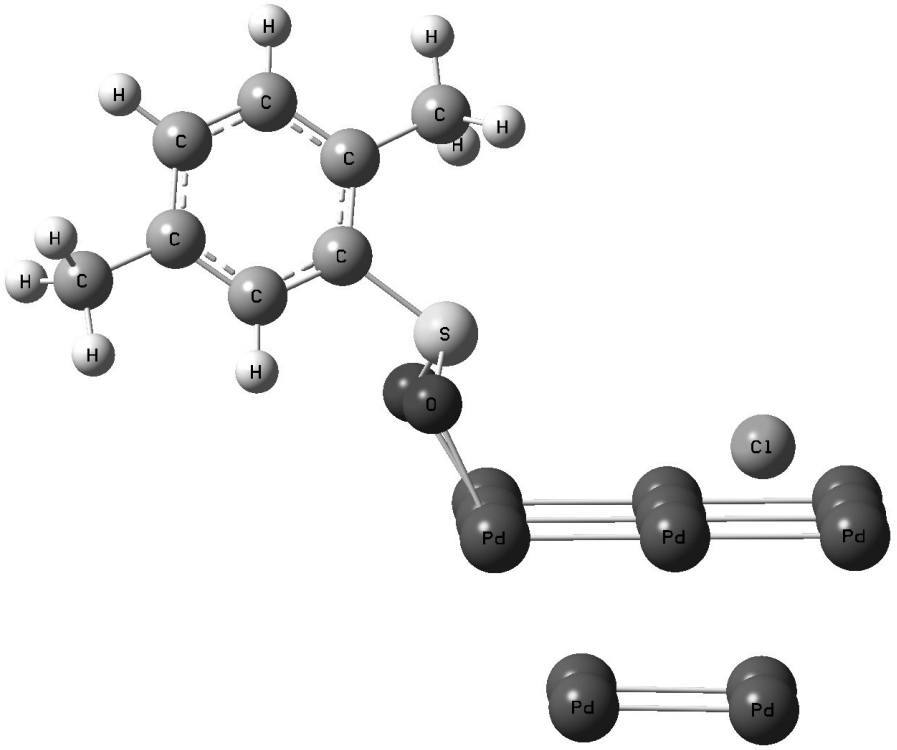


**Figure 3-9.** The results of the DFT optimization calculations over $Pd_{13}$. $\Delta H_{ads}$ = -56.92 kcal/mol. Charges on the various atoms across the three adsorption calculations from Figures 3-8a, 3-8b and 3-9 ranged as follows: Oxygen = -0.373 to -0.551 (avg. = -0.473); Chlorine = -0.109 to -0.133 (avg. = -0.124); Sulfur = 0.754 to 0.843 (avg. = 0.793); Palladium = -0.09 to 0.2 (avg. = 0.0625). All instances of negatively charged Pd atoms were located in single layered clusters.

The same trend was obtained for each adsorption: a migration of the molecules toward the edges of the model surfaces and a separation of the chlorine from the remainder of the molecule. Barone and Duca[24] have already shown with their calculations that not all palladium molecules in a simulated surface were equal. The calculations here support that assertion because of the movement of the adsorbed molecules to the edges where Barone and Duca[24] have shown the more active atoms to be. Additionally, it was inferred from general expertise in the area of hydrogenation and dehydrogenation catalysts that the majority of the catalytic activity occurs on the "edges" or in the

"cracks" of Pd/C type catalysts. That is, the activity was highest along the boundaries of the palladium layers.

The $Pd_6$ cluster showed the phenomenon of atoms moving "below" the simulated surface, but single-layer representations cannot be expected to predict multi-layer behavior. The simplest multi-layer cluster, $Pd_8$, provided the same molecule migration and chlorine separation trends while also keeping the absorbed molecules "above" the simulated surface. This phenomenon extended to the more complicated $Pd_{13}$ cluster. These adsorption calculations succeeded in predicting what was already suspected of happening.

The minimized structures indicated that separation of chlorine from the rest of the molecule was relatively easy on the catalyst surface. These results further proved that the initial reactant and the palladium catalyst cluster would move to favorable configurations for the first reaction step naturally. The solution of the quantum mechanical equations showed the simulated molecules moved into positions that were prepared for hydrogen adsorption and/or collision to form the initial reaction products.

### 3.5 - Adsorption of Other Reaction Species

*Small, Common Molecules*

Hydrogen, water and hydrochloric acid (HCl) are all small, common molecules that are either reactants or products of the hydrogenation reaction discussed here. Adsorption of

water and hydrogen has been widely studied. Though in the case of hydrogen, atom adsorption is the focus more than adsorption of molecular hydrogen. HCl specifically has been less studied, but the results of the adsorption minimizations performed in this work yield a predictable result since hydrochloric acid is a reaction product and is readily absorbed into aqueous phases. The result of HCl adsorption over $Pd_{13}$ can be seen in Figure 3-10.

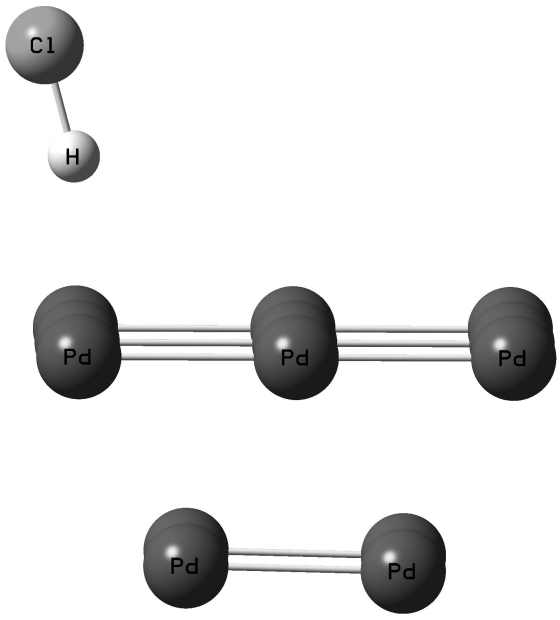


**Figure 3-10.** Hydrochloric acid adsorption results over the $Pd_{13}$ cluster. The minimizations show that the molecule remains intact rather than separating and moves away from the surface to a distance of approximately 3 Å. $\Delta H_{ads}$ = -5.73 kcal/mol.

When exposed to the palladium surface as a molecule, the tendency of the HCl is to back away from the surface and remain intact. This is in direct contradiction to the separation experienced by the chlorine atom in the initial 2,5-dimethyl benzene sulfonyl chloride molecule adsorption. The molecular binding energies of HCl are obviously stronger than those calculated in the sulfonyl chloride group. In this calculation HCl is weakly bound to the surface and is put in a position to be removed from the reaction sites easily. This fits in with the proposed reaction mechanism from DuPont[2] with HCl as a product of the initial reaction step and playing no further role in the hydrogenation.

Cao, et. al.,[54] shows that water binds weakly to Pd surfaces. Adsorption minimizations performed over $Pd_{13}$ have confirmed this fact. Water remained intact as a molecule with an adsorption distance of 2.51 Å from the oxygen atom. This is a distance at which it is easily removed from the surface in the toluene solvent system used for the hydrogenation reaction. It is believed that water from the dehydrations of sulfinic and sulfenic acid (reaction 2 from Figure 3-2) forms a second, aqueous liquid phase which is readily removed from the Pd reaction sites and sweeps the weakly bound HCl, a substance readily dissolved into aqueous solutions, with it. The results of the adsorption of water performed over the $Pd_{13}$ cluster is presented in Figure 3-11.

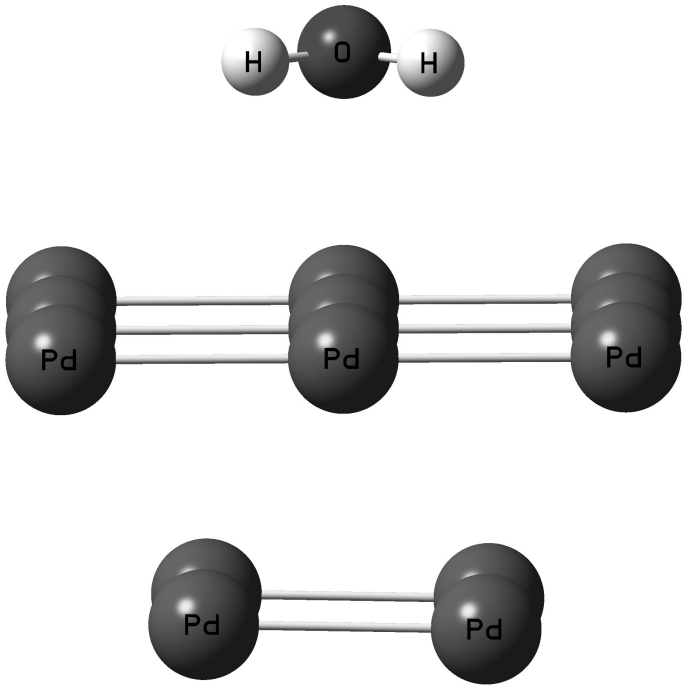


**Figure 3-11.** Adsorption of water over the $Pd_{13}$ cluster. Water remains intact and at a distance of approximately 2.5 Å. $\Delta H_{ads}$ = -9.42 kcal/mol.

Hydrogen adsorption to Pd surfaces is a widely studied event. Most of the computational chemistry studies have been with hydrogen atoms rather than molecules given gaseous hydrogen's propensity to separate over Pd surfaces. Work performed in this study was on molecular hydrogen and separated hydrogen atoms over the $Pd_{13}$ surface.

Molecular hydrogen showed interesting behavior over $Pd_{13}$. When the hydrogen ($H_2$) molecule was exposed to the Pd surface at standard adsorption distances used by other molecules in this study (2.5 - 3 Å), its behavior was to remain intact and move away from the surface, much like the adsorptions of water and HCl. This behavior is in direct

opposition to the studies done on hydrogen adsorption[55] and general knowledge of the behavior of hydrogen on Pd surfaces. Hydrogen is known not only to adsorb atoms to Pd surfaces but in some cases to adsorb into the Pd surfaces creating subsurface palladium-hydride compounds.[55] In these studies, due to the frozen position of the Pd atoms, sub-surface interactions of hydrogen atoms will not be seen. The $Pd_{13}$ cluster acts as a solid barrier surface upon which the various adsorptions and hydrogenation reactions occur, the individual Pd atoms simply do not have enough freedom of movement to allow surface penetrations of any type.

Further adsorption minimizations were performed on hydrogen over $Pd_{13}$ in three phases. They were adsorption of molecular hydrogen at close (1.5 Å) distances to the surface, adsorption of two separate hydrogen atoms at distances of greater than 1.5 Å from one another and greater than 2 Å from the Pd surface and finally, adsorption of a single hydrogen atom to the surface under adsorption conditions used with other species in this study. These studies showed that there are two regimes in the adsorption of $H_2$ molecules. At distances of less than 1.85 Å from the surface, the molecule is driven apart to adsorb separately into 2 individual atoms. At distances greater than 1.85 Å from the surface and when the hydrogen atoms are within 1 Å of one another the H-H bond reforms. From that point the $H_2$ molecule acts as water and HCl do on the Pd surface. If the individual hydrogen atoms are more than 1.5 Å apart, there is no tendency to reform the H-H bond no matter the distance from the Pd surface and the atoms adsorb readily to the Pd surface at distances of 2 – 2.5 Å. Even when put on the surface two at a time, if

the distances are 1.5 Å or greater, the hydrogen atoms behave as individuals rather than reforming $H_2$ molecules. In the adsorption studies using molecular hydrogen, separation of the molecule into individual atoms on the surface was determined to be a local energy minimum, but the global minimum was calculated by reforming the molecule and having it distance itself from the Pd surface. The difference in the energy minimums was 2.1 kcal/mol.

*Hydrogenation Product Adsorption*

2,5-dimethyl benzenethiol is the intended product of the overall hydrogenation reaction. This compound is the desired result of the mechanism provided in Figure 3-1, the marketable compound to be sold on the open market. Structural minimizations and adsorption minimizations over $Pd_{13}$ were performed on this molecule so that its role in the reaction and mechanism could be better understood. Figures 3-12, 3-13 and 3-14 show the results of these calculations.

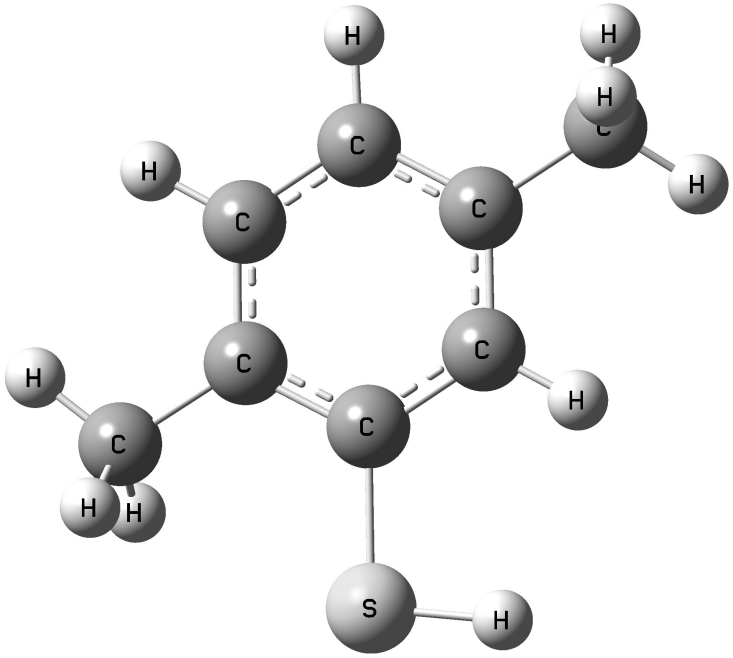


**Figure 3-12.** Structural DFT minimization of 2,5-dimethyl benzenethiol. Dipole moment = 1.204 Debye. C-S bond = 1.8 Å. S-H bond = 1.35 Å.

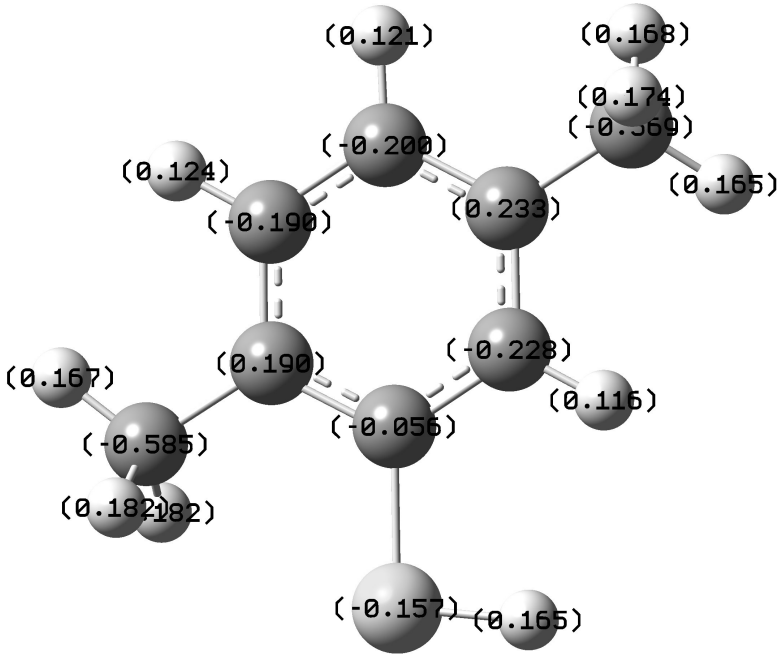


**Figure 3-13.** Charge distribution for the structural minimization of 2,5-dimethyl benzenethiol.

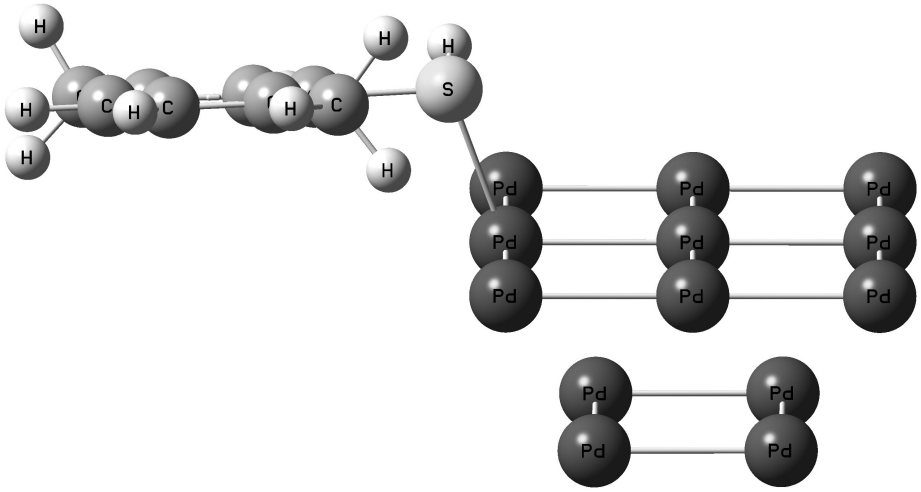


**Figure 3-14.** Adsorption minimization results for 2,5-dimethyl benzenethiol on $Pd_{13}$ cluster. $\Delta H_{ads}$ = -19.4 kcal/mol.

The reaction product shows a similar adsorption mode to the reactant in that it has bound to the edge of the surface and has interacted through atoms that are well known as Pd catalyst poisons. The difference in heat of adsorption between 2,5-dimethyl benzene sulfonyl chloride and 2,5-dimethyl benzenethiol shows that thiol doesn't bind as strongly to the catalyst surface intact after forming than does the sulfonyl chloride. This agrees with the expected result. Though the binding energies are not as low as those exhibited by water and HCl, they are the lowest of any aromatic molecule in the study of this reaction.

*Intermediate Molecule Adsorption*

2,5-dimethyl benzene sulfinic acid, 2,5-dimethyl benzene sulfenic acid and 2,5 dimethyl benzene disulfide are all important intermediates of the reactions shown in Figures 3-1 and 3-2. The sulfenic acid is not shown as one of the underlying steps in reaction 2 in Figure 3-2 going from the sulfinic acid to the disulfide. After one dehydration step the sulfinic acid becomes the sulfenic acid. After another dehydration step the sulfenic acid becomes one-half of the disulfide molecule. Structural minimizations and subsequent adsorption minimizations over $Pd_{13}$ were performed with each molecule and the results are shown in Figures 3-15 through 3-23.

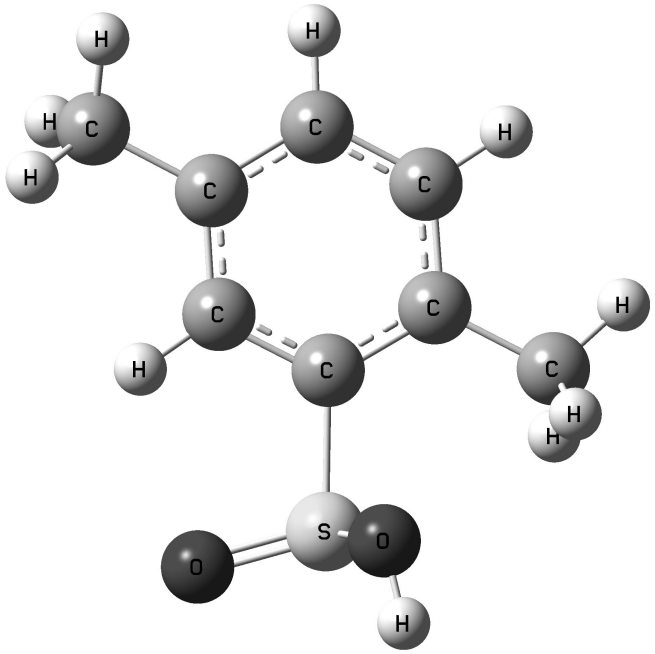


**Figure 3-15.** Structural DFT minimization of 2,5-dimethyl benzene sulfinic acid. Dipole moment = 2.76 Debye. C-S bond = 1.82 Å. S=O bond = 1.5 Å. S-O bond = 1.725 Å. O-H bond = 0.97 Å.

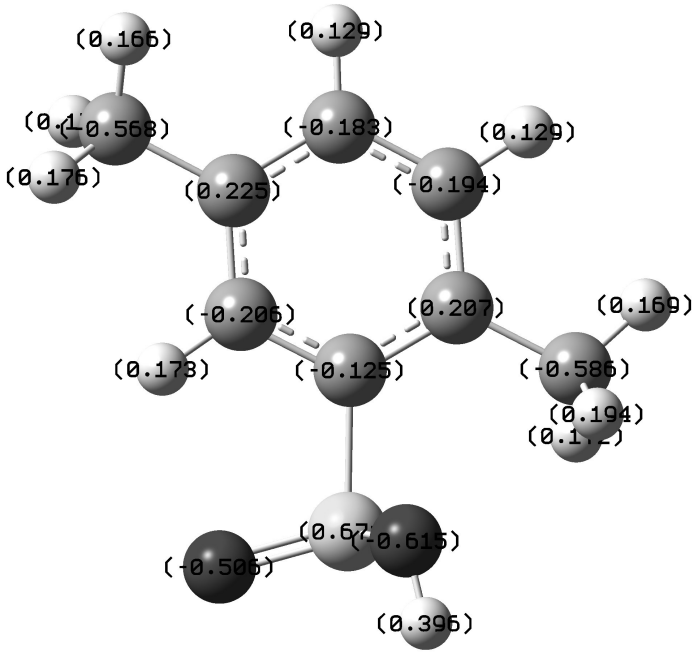


**Figure 3-16.** Charge distribution for the structural minimization of 2,5-dimethyl benzene sulfinic acid. Difficult to read charges on the oxygen atoms are -0.505 for the =O group and -0.615 for the –OH group, respectively.

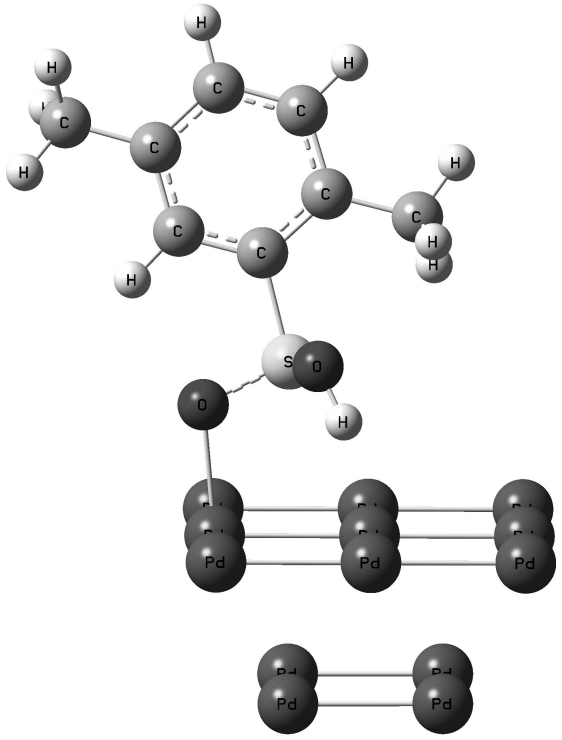


**Figure 3-17.** Adsorption minimization for 2,5-dimethyl benzene sulfinic acid on $Pd_{13}$ cluster. $\Delta H_{ads}$ = -23.9 kcal/mol.

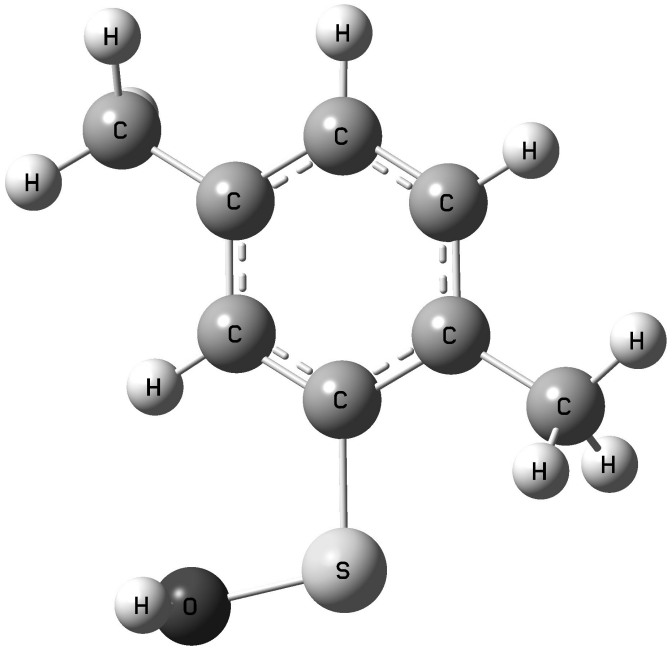


**Figure 3-18.** Structural DFT minimization of 2,5-dimethyl benzene sulfenic acid. Dipole moment = 1.925 Debye. C-S bond = 1.8 Å. S-O bond = 1.7 Å. O-H bond = 0.97 Å.

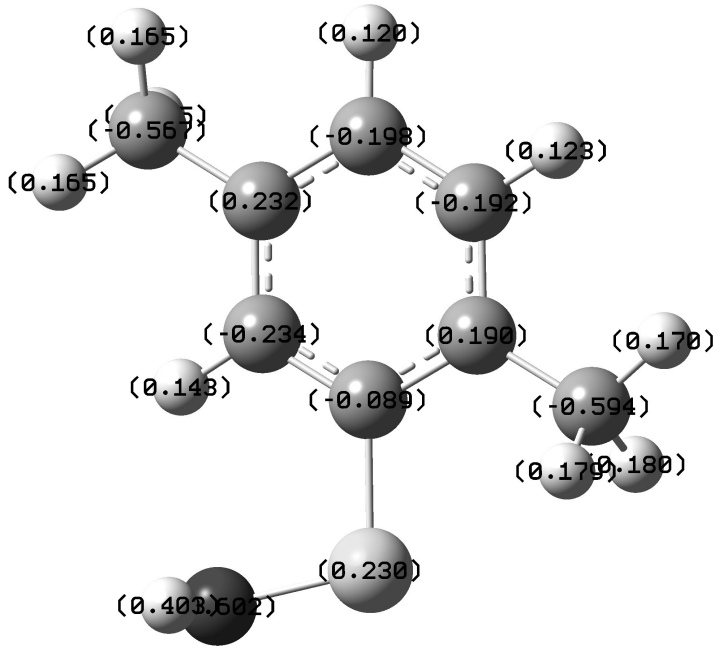


**Figure 3-19.** Charge distribution for the structural minimization of 2,5-dimethyl benzene sulfenic acid. Difficult to read charges on the –OH group are -0.602 for the oxygen and 0.403 for the hydrogen respectively.

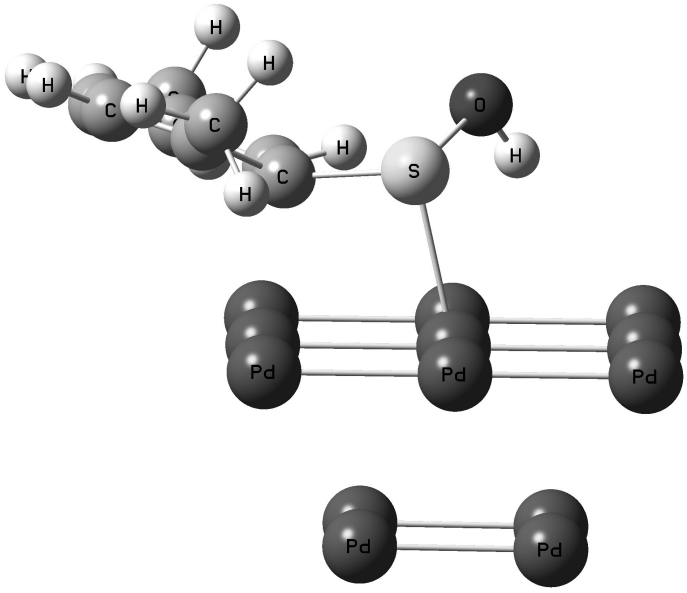


**Figure 3-20.** Adsorption minimization for 2,5-dimethyl benzene sulfenic acid on $Pd_{13}$ cluster. $\Delta H_{ads}$ = -28.1 kcal/mol.

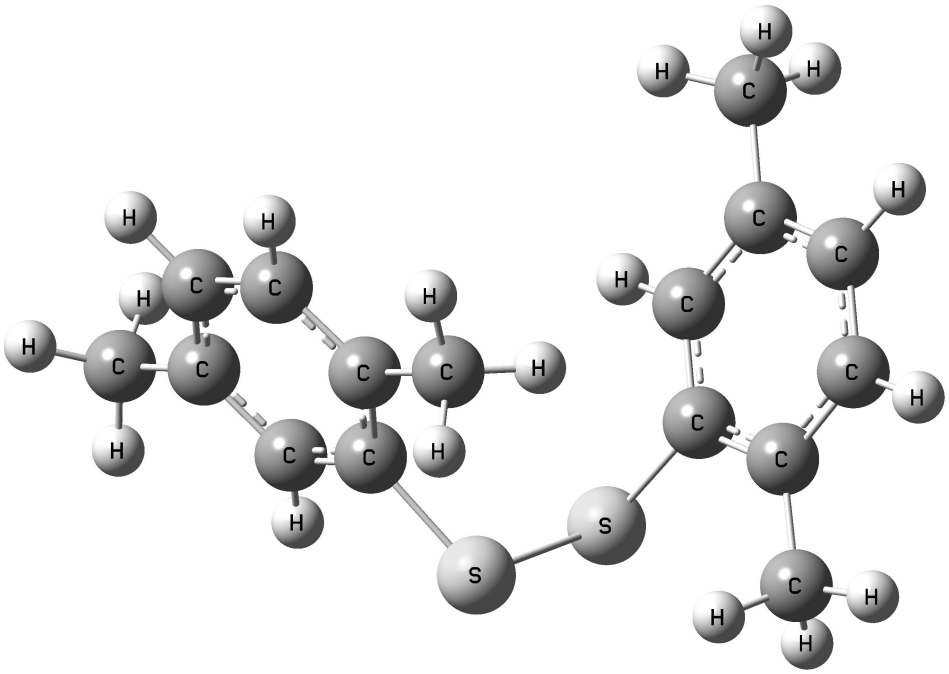


**Figure 3-21.** Structural DFT minimization of 2,5-dimethyl benzene disulfide. Dipole moment = 2.73 Debye. C-S bond #1 = 1.8 Å. C-S bond #2 = 1.8 Å. S-S bond = 2.13 Å. C-S-S-C dihedral = $81.6^0$

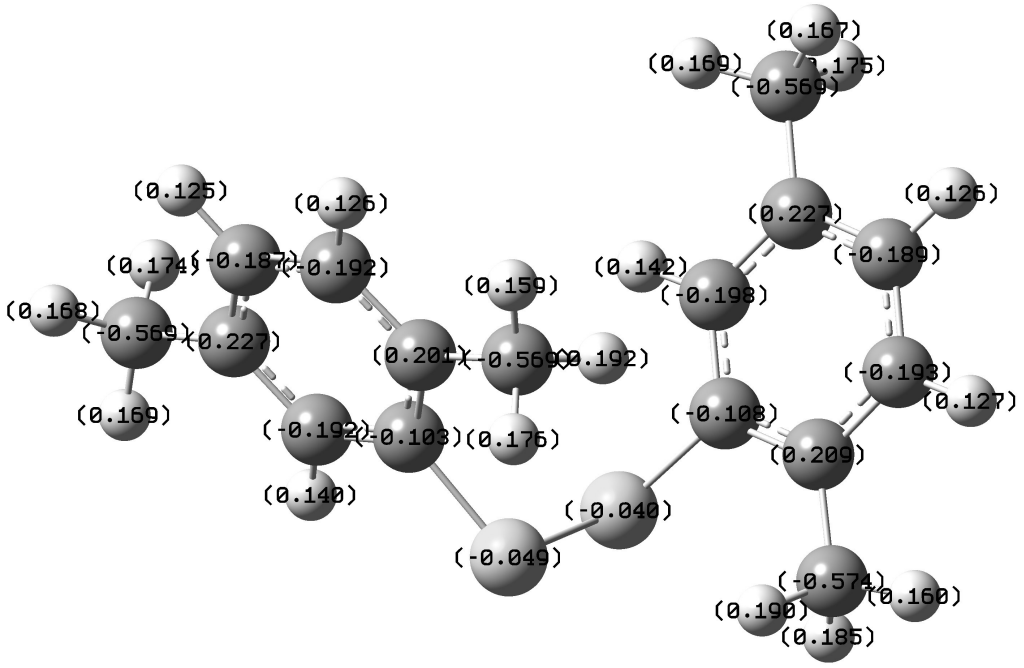


**Figure 3-22.** Charge distribution for the structural minimization of 2,5-dimethyl benzene disulfide.

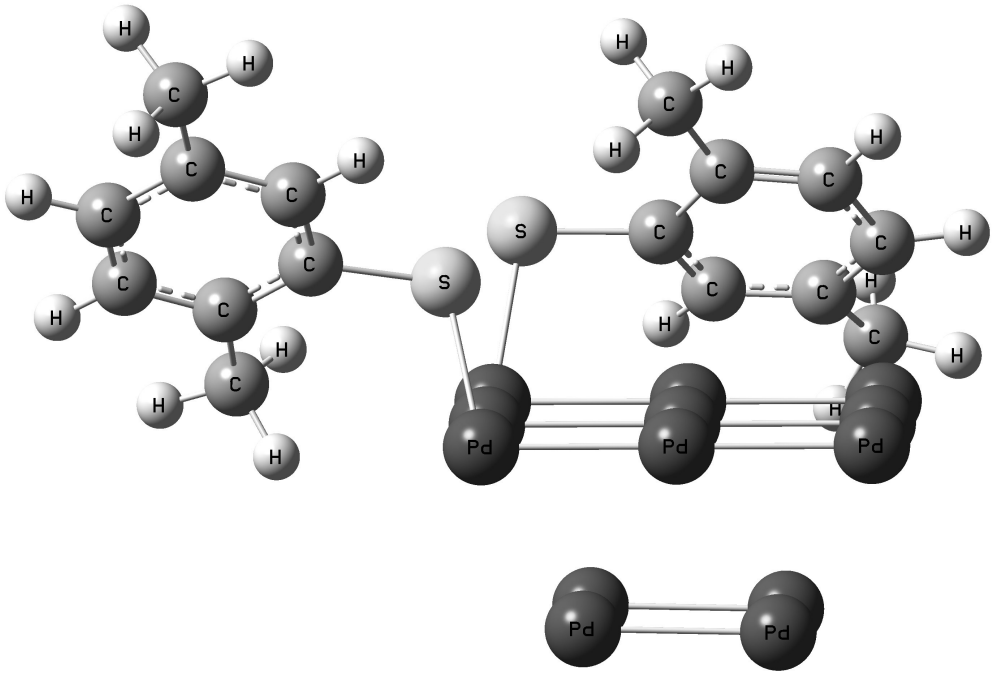


**Figure 3-23.** Adsorption minimization for 2,5-dimethyl benzene disulfide on $Pd_{13}$ cluster. $\Delta H_{ads}$ = -64.5 kcal/mol.

Figure 3-17 shows a logical progression from Figure 3-9 through the proposed reaction mechanism from DuPont shown in Figure 3-2. The progression from Figure 3-9 to Figure 3-17 is the addition of hydrogen to one of the formerly Pd-bound oxygen atoms on the molecule. Not shown in Figure 3-17 is the presumed HCl formation and subsequent release from the surface which if included would complete reaction 1 from Figure 3-2. Reaction 2 from Figure 3-2 is a bit more complicated. The first step is a dehydration reaction to go from sulfinic acid in Figure 3-17 to sulfenic acid in Figure 3-20. Adsorption minimizations of each of those molecules show a shift in the binding of the molecule from the oxygen atom(s) to interaction through the sulfur atom. This is an

important step that was expected to occur so that the sulfenic acid can easily undergo a second dehydration step leaving behind one-half of the disulfide molecule. The higher binding energies of sulfur to Pd surfaces than oxygen, discussed in an earlier section, allow the adsorption to take place at the more weakly active center Pd atom rather than on the edges as has been previously seen in all molecules. Additionally, Figure 3-23 shows the interesting phenomena of adsorption of 2,5-dimethyl benzene disulfide with dissociation. This type of adsorption behavior has been seen in other aromatic disulfide compounds when using the disulfide bond to adsorb onto the surface rather than some other adsorption modes utilizing different bonds.[56] This type of adsorption has the added benefit of having the disulfide already prepared on the surface for a reaction with adsorbed hydrogen to readily form the reaction product, 2,5-dimethyl benzenethiol. The dehydration reaction of 2,5-dimethylbenzene sulfenic acid, the adsorbed molecule is

shown in Figure 3-20, also results in an adsorbed molecule that is equivalent to one-half of the adsorbed 2,5-dimethylbenzene disulfide.

The molecule formed by adsorption of 2,5-dimethylbenzene disulfide and the dehydration of the 2,5-dimethylbenzene sulfenic acid was dubbed the thiol anion. Given the form of the thiol anion, why must it go through the formation of the disulfide bond, as proposed in Figure 3-2, rather than simply reacting with adsorbed hydrogen to form 2,5-dimethylbenzenethiol? A shift in the reaction pathway based on these observations would make 2,5-dimethylbenzene disulfide a by-product rather than an intermediate. .

### 3.6 - An Alternative Reaction Pathway

If disulfide is a by-product of the reaction then how does the new reaction mechanism look when compared to Figure 3-2? The new pathway is presented in Figure 3-24.

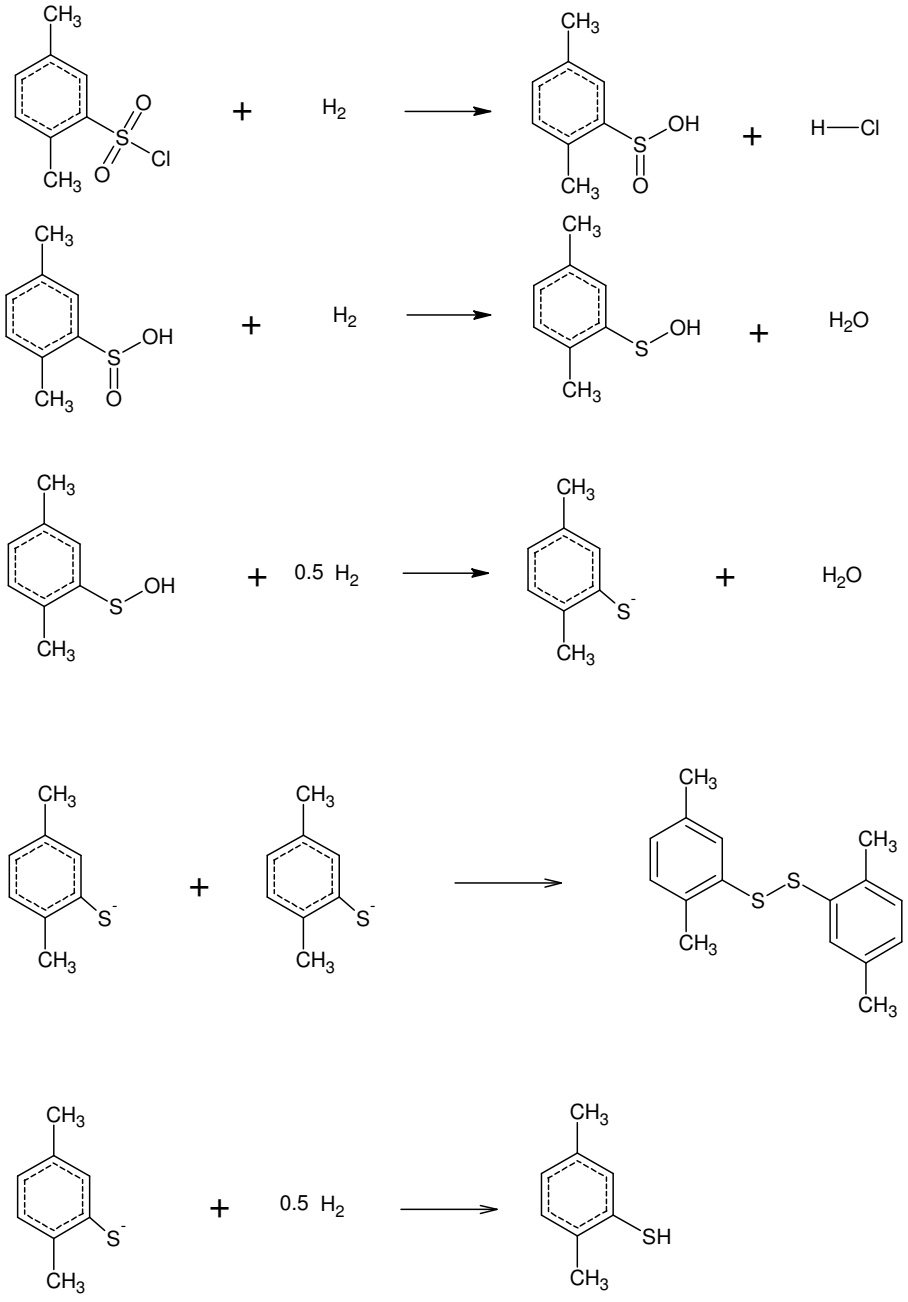


**Figure 3-24.** A proposed alternative reaction pathway for the hydrogenation of 2,5-dimethyl benzene sulfonyl chloride. The pathway also goes to the product structure, 2,5-dimethyl benzene thiol, through the "thiol anion" structure as based on DFT calculations performed on the adsorption of all reaction species over the $Pd_{13}$ cluster.

To be able to properly compare this reaction pathway to the one that DuPont proposes, an additional set of structural minimizations and adsorption calculations must be performed on the thiol anion structure. The results are shown in Figures 3-25, 3-26 and 3-27.

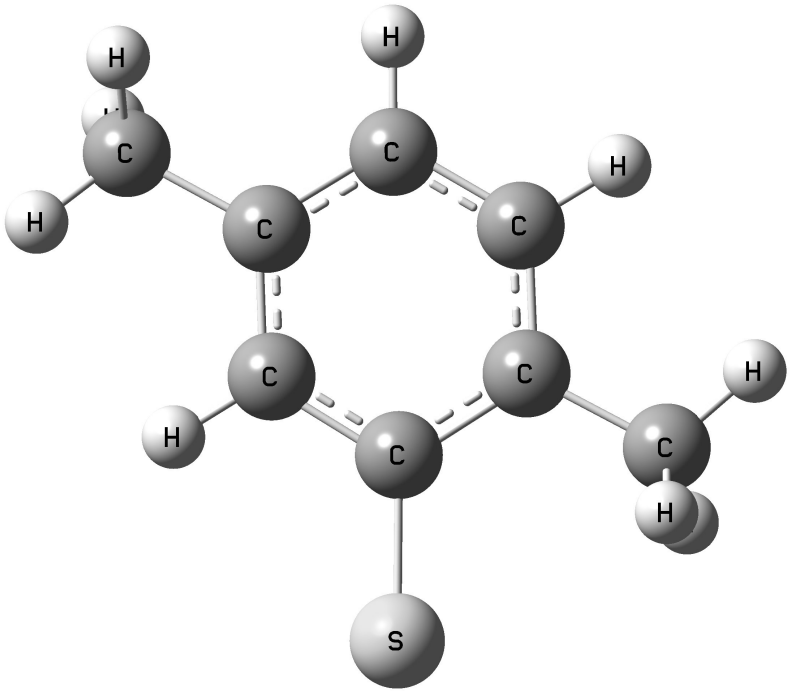


**Figure 3-25.** Structural DFT minimization of 2,5-dimethyl benzenethiol anion. Dipole moment = 6.33 Debye. C-S bond = 1.756 Å. The overall charge of this molecule is -1.

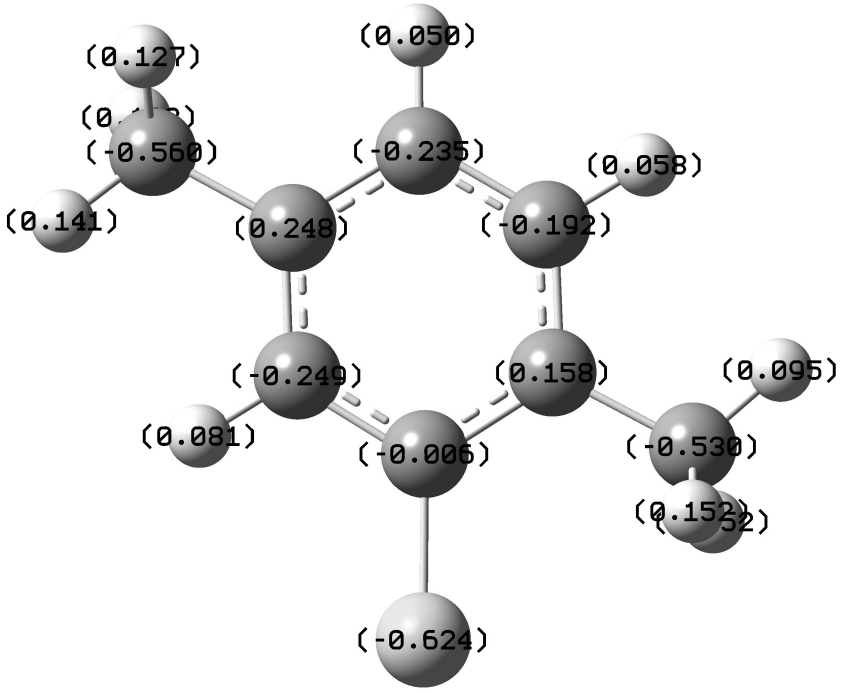


**Figure 3-26.** Charge distribution for the structural minimization of 2,5-dimethyl benzenethiol anion. Notice that the sulfur atom is highly negatively charged in this instance.

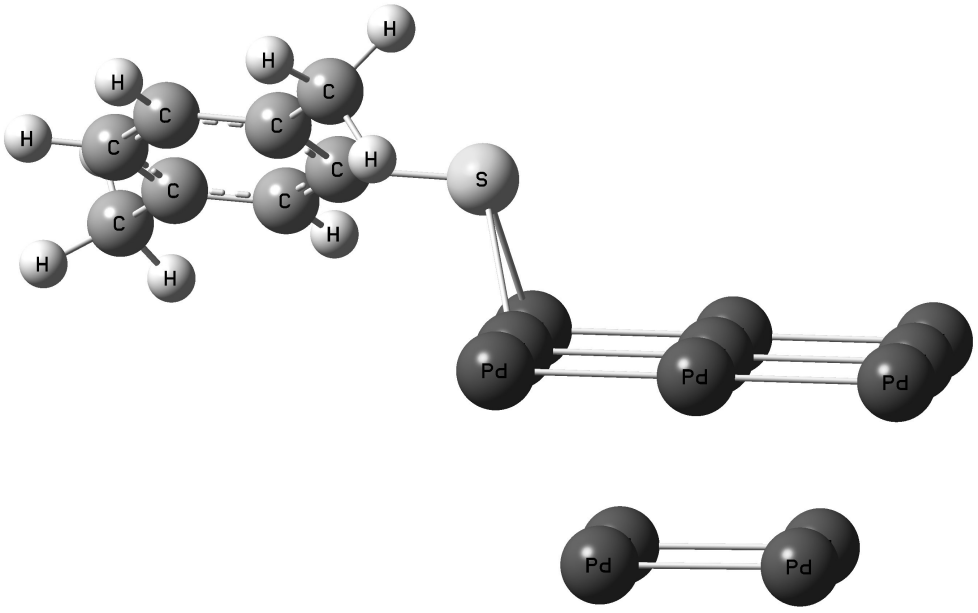


**Figure 3-27.** Adsorption minimization for 2,5-dimethyl benzenethiol anion on $Pd_{13}$ cluster. $\Delta H_{ads}$ = -76.1 kcal/mol.

Figure 3-27 shows encouraging signs of being a step in the right direction for a reaction pathway. The difference between it and Figure 3-14 (benzenethiol adsorption) are minimal at best. Each has adopted very similar configurations with the only difference being that Figure 3-14 shows an S-H bond where Figure 3-27 shows an S-Pd bond in its place. Figure 3-27 is also comparable to Figures 3-20 and 3-23 when adsorption mode is considered. It is not difficult to see how the reaction pathway could pass through the thiol anion species. Further calculation to confirm the initial observations was still needed however.

Frequency calculations on all species in each reaction pathway were performed. These calculations returned values that allowed the Gibbs Free Energy of reaction ($\Delta G_{rxn}$) to be determined for each individual reaction step. The results are shown in Table 3-2.

**Table 3-2.** A listing of the Gibbs Free Energies of the two alternative reaction pathways. Reaction number under the DuPont pathway refers to Figure 3-2, while reaction number under the alternate pathway refers to Figure 3-24. $\Delta G_{rxn}$ are calculated from energies calculated from frequency calculations of DFT structural and adsorption minimizations performed on each reaction species in the individual pathways.

| DuPont Pathway | $\Delta G_{rxn}$ kcal/mol | Alternate Pathway | $\Delta G_{rxn}$ kcal/mol |
|---|---|---|---|
| Reaction 1 | -18.82 | Reaction 1 | -24.9 |
| Reaction 2 | -84.67 | Reaction 2 | -37.77 |
| Reaction 3 | -10.85 | Reaction 3 | -33.37 |
| | | Reaction 4 | 78.43 |
| | | Reaction 5 | 133.85 |

As Table 3-2 clearly demonstrates, while the alternative pathway using the thiol anion as an intermediate and forming the disulfide species as a by-product looks feasible when viewing the behaviors of the molecules on the Pd surface, the thermodynamics do not confirm that theory. Any reaction with the thiol anion as a reactant has a positive $\Delta G_{rxn}$ which means that the reactants of the reaction are preferred thermodynamically to the products. Unfortunately, with such large positive values for the reactions, it is improbable that they would ever occur. The thermodynamics simply do not favor the alternate reaction pathway proposed earlier. Meaning that the disulfide is indeed an

intermediate and that the proposed reaction sequence from Figure 3-2 is the most feasible submitted to date.

### 3.7 - Conclusions

The adsorption and minimization steps included here are a good start toward understanding the mechanism of the hydrogenation reaction. The adsorption steps indicated that chlorine separation from the rest of the initial reactant molecule is not difficult on the catalyst surface. The investigation also shows that the reaction species, in most cases, interacts more readily with the edges of the Pd clusters rather than the centers. Additionally, the progression of the adsorption minimizations through the rest of the reaction species provided no surprises or alternative pathways that diverged from the initially predicted hydrogenation reaction pathway. The next step would be to start calculations that would lead to activation energy results that may be compared with current experimental data.

# 4. TRANSITION STATE CALCULATIONS

## 4.1 - Introduction

A transition state is defined as a molecular configuration along a reaction coordinate that corresponds to the highest energy along that coordinate.[57] The energy barrier through the transition state must be overcome in order for a chemical reaction to occur. The energy barrier is commonly referred to as the activation energy ($E_a$). Quantum mechanical simulations can be used to determine transition state structures even though the rules of quantum mechanics prevent actual observation of the transition state in reality.

In scanning a potential energy surface of a given set of atoms the transition state can be located. The transition states are described as first-order saddle points as shown in Figure 4-1. Quadratic Synchronous Transit-Guided Quasi-Newton (QST2 and QST3) simulation types, a sub-routine within Gaussian,[16] allow one to scan a given potential energy surface between reactant and product structures for first-order saddle points to determine transition states. This process is often problematic but generally proceeds as follows. First, the reactant and product structures must be minimized to stable energy states. Then, the QST input files are created by incorporating the minimized reactant and product structures. In the case of QST2 the simulation will generate an initial guess between the two reaction structures for the transition state and the search for the first-order saddle point will commence. In the case of QST3 the initial guess for the transition state structure is supplied by the user. QST3 calculations are often used if empirical data on the transition state is known or if previous calculations have been performed on the

particular reactant-product system and the user wants to restart calculations from a point in a previous job. The results from a QST calculation are used for a frequency calculation to verify that they are indeed a first-order saddle point and further used for an Intrinsic Reaction Coordinate (IRC) calculation to verify that the reaction coordinate which the first-order saddle point lies on is the one that the user desires. Frequency and IRC calculations simply insure that the results obtained are a true transition state for the desired reaction pathway.

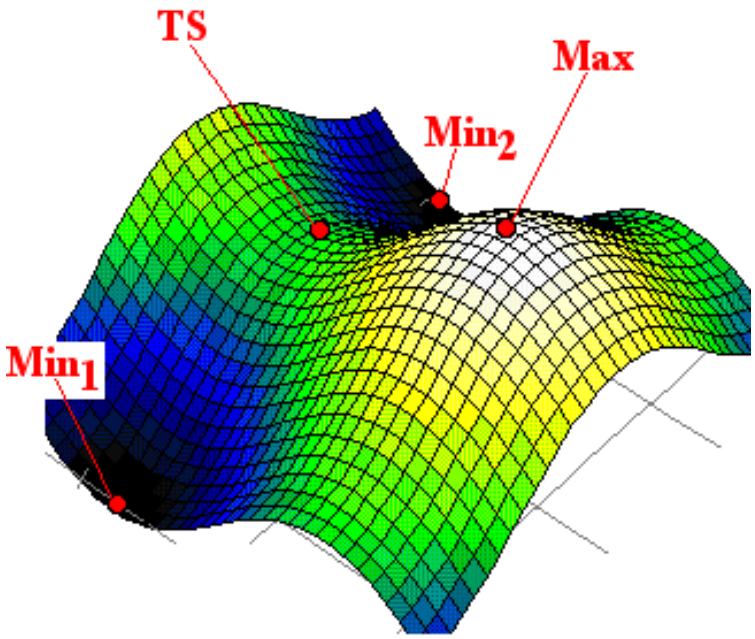


**Figure 4-1.** A general representation of a 3-dimensional potential energy surface. The points of emphasis are showing a first-order saddle point corresponding to a transition state. The points Min1 and Min2 correspond to user minimized reactant and product structures. The direction of the reaction, as to whether Min1 corresponds to reactant or product and Min2 the other, depends on the particular reaction. Taking a vertical "slice" out of the 3-D potential energy surface that intersects all three points (Min1, Min2 and TS) provides a 2-D picture that is more prevalent in transition state discussions.

The 2-D representation is shown in Figure 4-2.

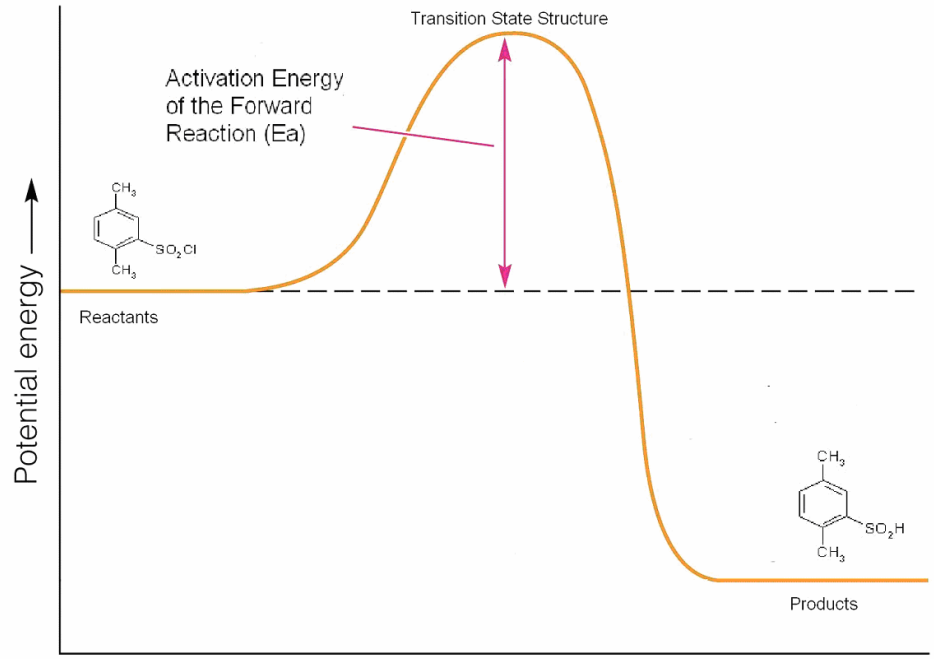


**Figure 4-2.** A 2-D representation of the potential energy surface depicting a transition state.

*The Transition State of the Hydrogenation of 2,5-Dimethylbenzene Sulfonyl Chloride*

DuPont's investigation into the hydrogenation technology discussed in this paper showed that the kinetics of the reaction is well represented by a first order reaction with 2,5-dimethylbenzene sulfonyl chloride as the substrate.[2] The only reaction utilizing the sulfonyl chloride molecule on either side of the reaction in the proposed reaction pathway, shown in Figure 3-2, is the initial reaction step converting 2,5-dimethylbenzene sulfonyl chloride to 2,5-dimethylbenzene sulfinic acid. For that reason,

that step was chosen as the rate-limiting step for the purposes of finding the transition state through computational means.

Following the general strategy of finding transition states through computational means described above, the reactant and product structures were minimized. Given the results presented in the previous section on the adsorption of 2,5-dimethyl benzene sulfonyl chloride on three different Pd (100) surfaces, there are three different starting points. Transition states were determined over all three surfaces ($Pd_6$, $Pd_8$ and $Pd_{13}$) and the results were compared to values given for $E_a$ in the DuPont literature.[2] The final results from the adsorption calculations over all three Pd clusters were used and hydrogen was added in two different ways to create reactant and product structures, six total structures. After all reactant and product structures were structurally minimized three QST2 calculations were created and run. One QST-type simulation was completed for each Pd cluster. The final results from those calculations were run through frequency and IRC calculation checks. The results were compared to given experimental values. The results of the $E_a$ determination are shown in Table 4-1 and the details are discussed below.

**Table 4-1.** A listing of the various activation energies ($E_a$) calculated for the proposed rate-limiting step. The calculations for the rate limiting step of the hydrogenation of 2,5-dimethylbenzene sulfonyl chloride to 2,5-dimethylbenzenethiol were done either experimentally or through quantum mechanical (QST2/QST3) calculations.

| Data Source | DuPont Exp. | $Pd_6$ Simulation | $Pd_8$ Simulation | $Pd_{13}$ Simulation |
|---|---|---|---|---|
| $E_a$ (kcal/mol) | 14.58 | 6.88 | 38.1 | ~10-20 |

### 4.2 - Reactant Species Creation and Minimization

The adsorbed forms of 2,5-dimethylbenzene sulfonyl chloride over all three Pd clusters can be seen in Figures 3-8a, 3-8b and 3-9. All adsorption minimizations showed dissociation of the chlorine atom from the rest of the aromatic component and in particular the case of $Pd_8$ shows that the two portions of the benzene sulfonyl chloride molecule move to complete opposite ends of the cluster upon adsorption. In order to create actual reactant structures from these adsorption minimizations, molecular hydrogen must be added at a strategic spot in the overall structure to facilitate the 2,5-dimethylbenzene sulfonyl chloride to 2,5-dimethylbenzene sulfinic acid reaction. The initial guess for the position of the insertion of molecular hydrogen must be reasonable. The structural minimization of the adsorption results with the additional hydrogen provided the reactant structure that was used for the initial QST2 calculation for each Pd cluster and also for each subsequent QST3 calculation to guarantee consistency of results. The results of the reactant minimizations are presented in Figures 4-3, 4-4 and 4-5.

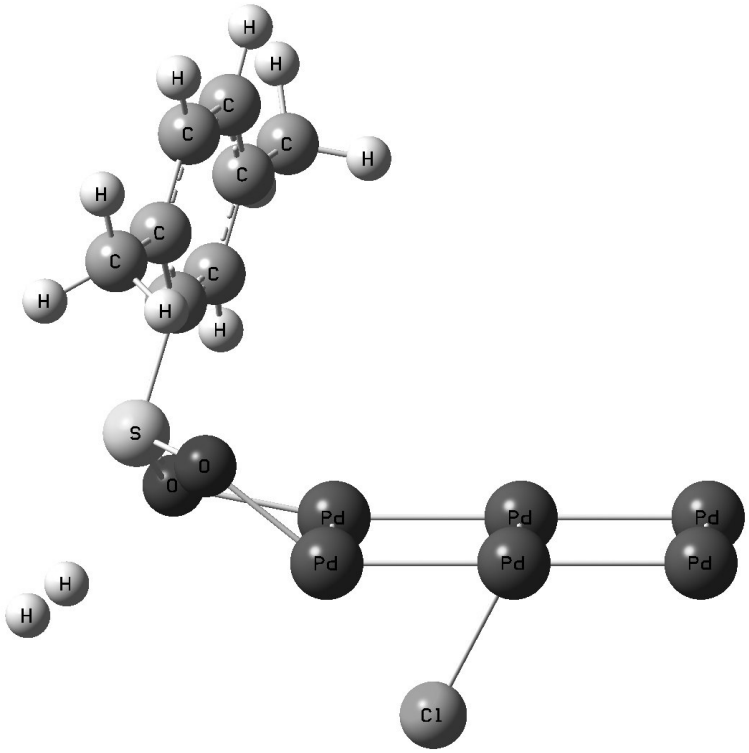


**Figure 4-3.** The minimized reactant structure over $Pd_6$.

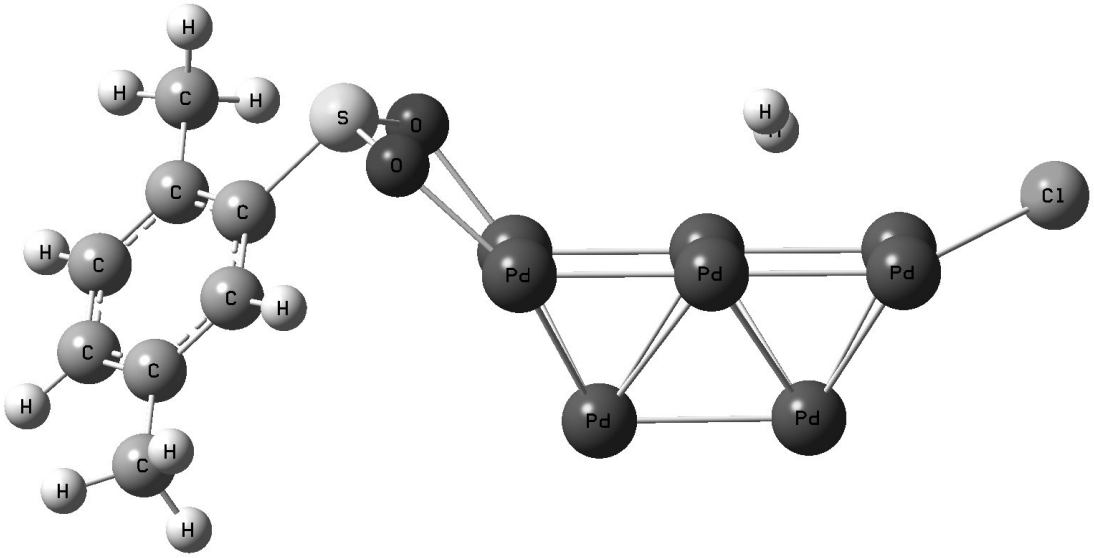


**Figure 4-4.** The minimized reactant structure over $Pd_8$.

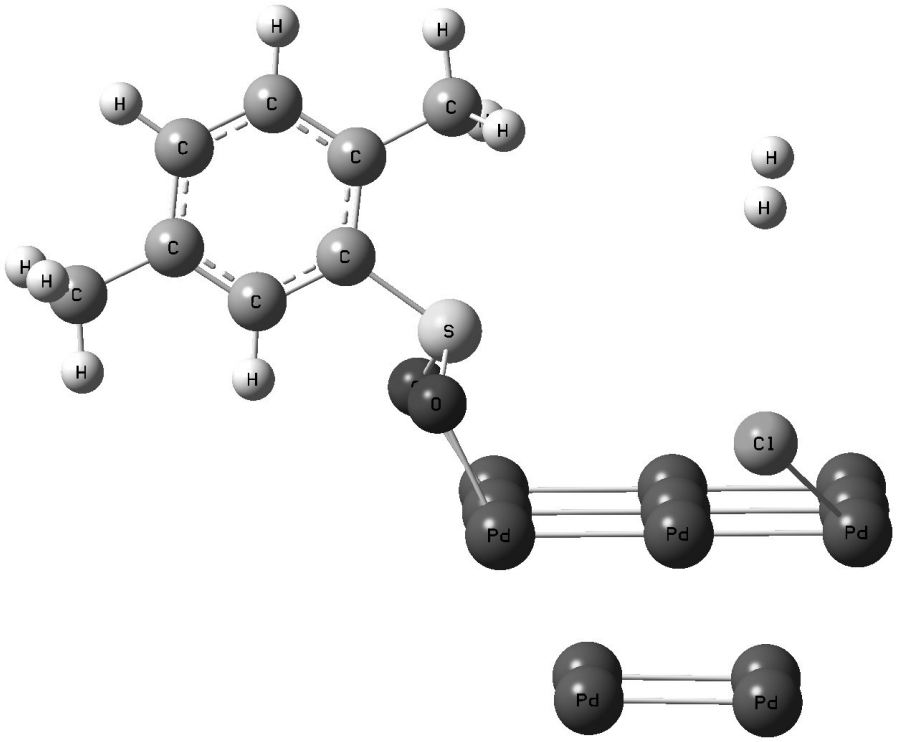


**Figure 4-5.** The minimized reactant structure over $Pd_{13}$.

One can see that the minimized reactant structures when compared to their matching adsorption structures in Figures 3-8a, 3-8b and 3-9 do not vary greatly except in the addition of a molecule of hydrogen. The above reactant structures were used for the input into each respective QST calculation.

### 4.3 - Product Species Creation and Minimization

In the same way that reactant species were created by adding molecular hydrogen to adsorption minimizations, product species were created by adding hydrogen atoms bound to specific locations on the adsorbed molecule. The hydrogen atoms at these

locations created the products from the proposed rate-limiting step in the reaction, 2,5-dimethylbenzene sulfinic acid and hydrochloric acid. The newly created molecules were then structurally minimized. The results provided structures to represent adsorbed molecules on the three Pd clusters that were suitable to include as product structures in QST calculations. The minimized structures are shown in Figures 4-6, 4-7 and 4-8.

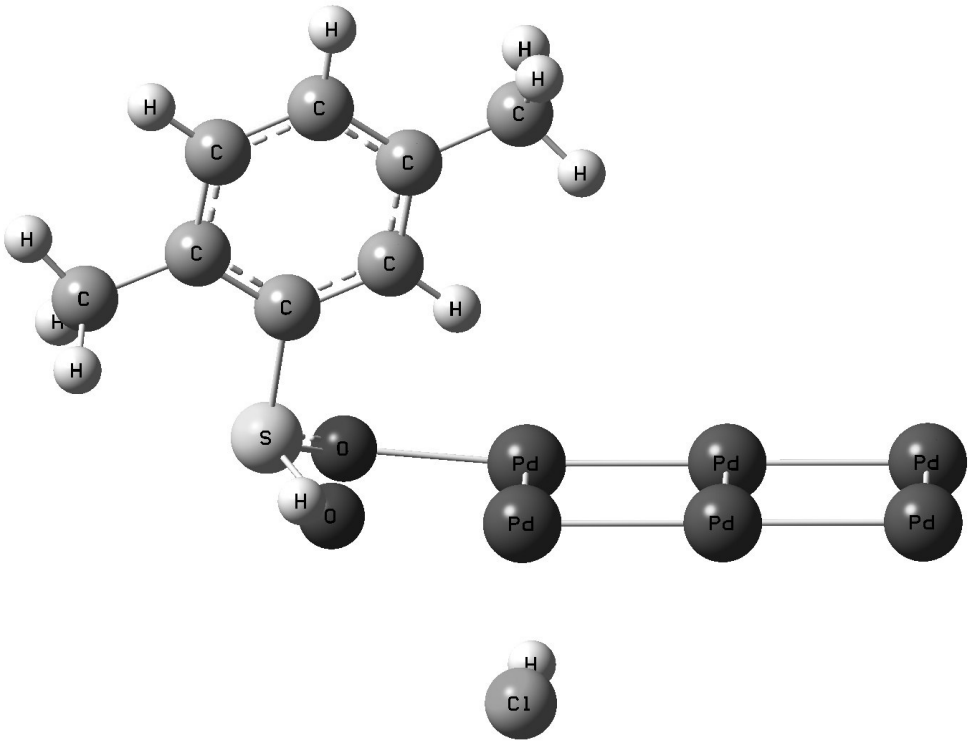


**Figure 4-6.** The minimized product structure over $Pd_6$.

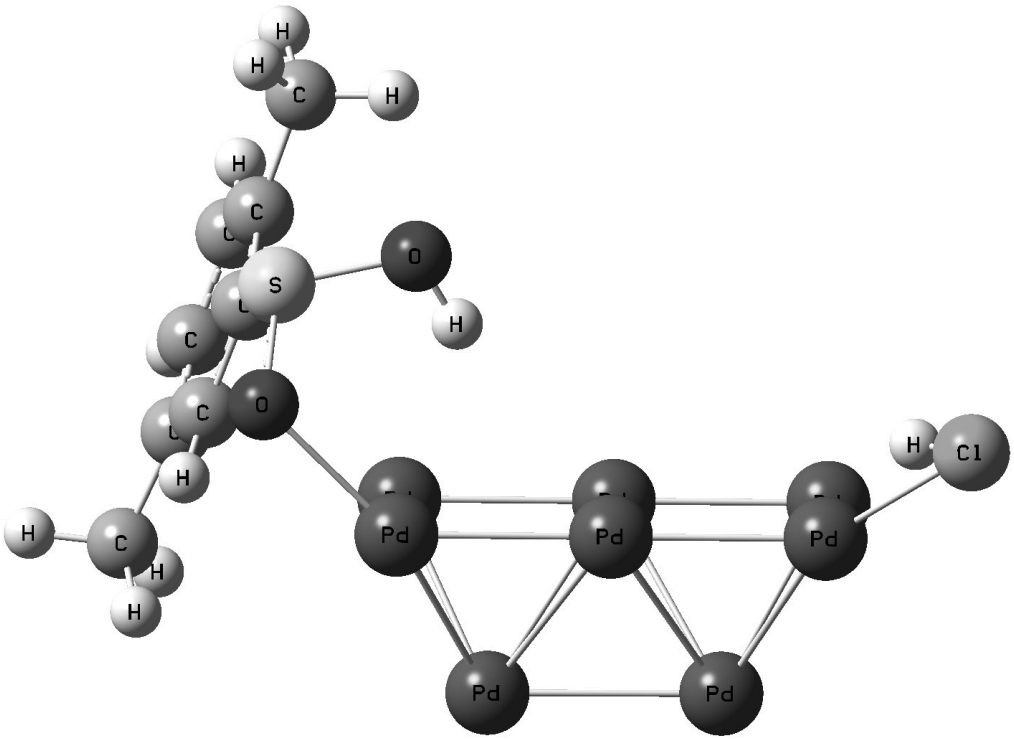


**Figure 4-7.** The minimized product structure over $Pd_8$.

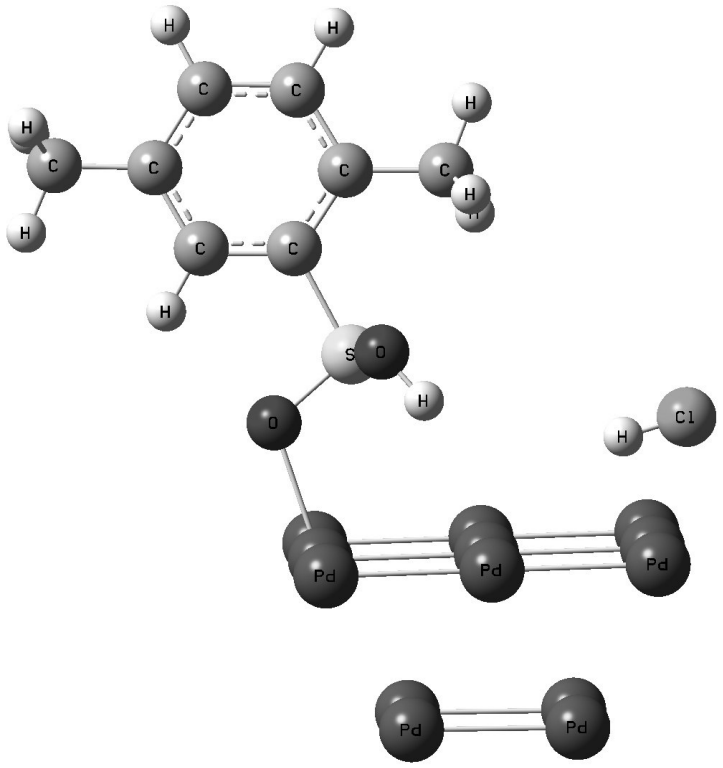


**Figure 4-8.** The minimized product structure over $Pd_{13}$.

There are significant changes between the adsorbed forms of the 2,5-dimethylbenzene sulfonyl chloride and the molecules shown in the product structures, but that is expected. The molecular bonds have changed and with them the charges and forces influencing the adsorbed molecules result in the structures seen above. However, when the sulfinic acid adsorption on $Pd_{13}$, from Figure 3-17 is compared to the product structure in Figure 4-8 the similarities are obvious. The product structures pictured above were used for their respective QST calculations and the calculations were allowed to run to completion.

### 4.4 - Results of the Transition State Calculations

Each transition state result was scrutinized carefully as it progressed to make sure that the purely computational approach utilized was remaining within the bounds of logical chemical reasoning. The results of all three first-order saddle point searches summarized in Table 4-1 above are presented below with more detail and insight into the reasoning used to interpret the results of the calculations. Individual activation energies ($E_a$) are calculated by finding the enthalpy change between the minimized reactant structure and the calculated transition structure. The first calculated transition state structure over $Pd_6$ is shown in Figure 4-9.

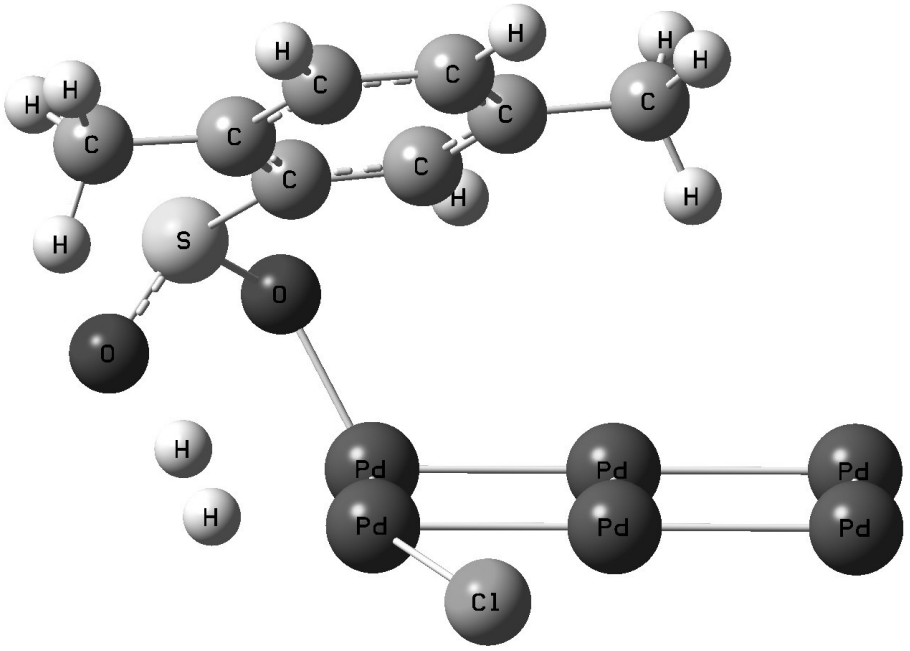


**Figure 4-9.** The calculated transition state structure over $Pd_6$. More specifically, this is the transition state for the conversion of 2,5-dimethylbezene sulfonyl chloride to 2,5-dimethylbenzene sulfinic acid and hydrochloric acid using $Pd_6$ as the simulated catalyst cluster. $E_a$ = 6.88 kcal/mol.

The calculated transition state using the $Pd_6$ cluster under-predicts the experimental value for $E_a$, though the transition state structure is logical given the progress of the reaction from reactants to products. The reasons for the $E_a$ calculation under-predicting the value were theorized to be due to the single layer construction of this particular cluster. The fact that the chlorine molecule has shifted "below" the given palladium surface allows the hydrogen to collide at a more efficient angle, that is, coming in from the outside to react with the "corner" of the catalyst cluster. The multi-layer Pd clusters are not able to take advantage of this behavior and the hydrogen molecules follow more difficult and energy intensive paths of reaction. Also the spacing for collision/reaction

requires less energy to achieve by allowing the chlorine to adsorb below the proposed Pd surface. These two energy-saving behaviors, which are not present in the actual Pd/C catalyst surface, allow the simulation to calculate an energy barrier that is less than the experimental data. The transition state calculated over $Pd_8$, shown in Figure 4-10, has the opposite result.

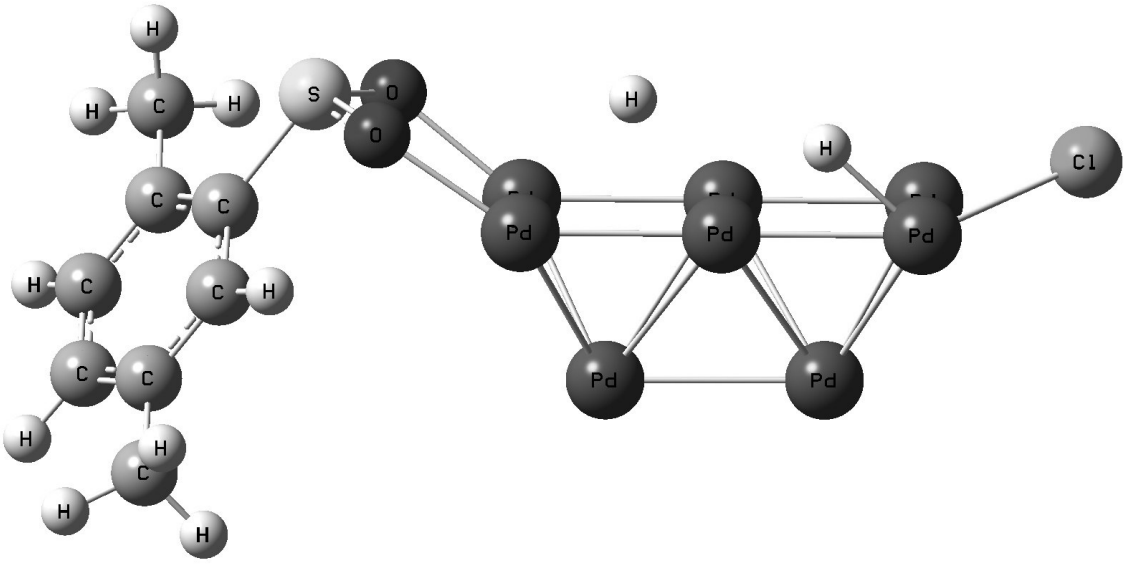


**Figure 4-10.** The calculated transition state structure over $Pd_8$. More specifically, this is the transition state for the conversion of 2,5-dimethylbezene sulfonyl chloride to 2,5-dimethylbenzene sulfinic acid and hydrochloric acid using $Pd_8$ as the simulated catalyst cluster. $E_a$ = 38.1 kcal/mol.

The calculated transition state using the $Pd_8$ cluster over-predicts the experimental value for $E_a$, though the transition state structure is logical for the starting and ending structures that were used in the calculations. The reasons for the energy barrier being so high in this example are due to the initial configuration of the 2,5-dimethylbenzene sulfonyl chloride adsorption. In hindsight, the $Pd_6$ and $Pd_8$ catalyst clusters are barely large enough to handle the simulation of such a large, complicated molecule as 2,5-dimethylbenzene with sulfur-containing functional groups. The initial adsorption of the reactant molecule onto $Pd_8$ provided a structure where the aromatic portion of the molecule and the chlorine atom were separated by a relatively long distance with several intervening adsorption sites between the two parts of the original molecule. The barriers for the adsorbed hydrogen atoms to overcome these intervening adsorption sites and move from the minimized reactant structure to the minimized product structure are thus added into the overall energy barrier predicted by the QST calculation. The calculated transition state over $Pd_{13}$, shown in Figure 4-11, provided yet a third type of result to be analyzed.

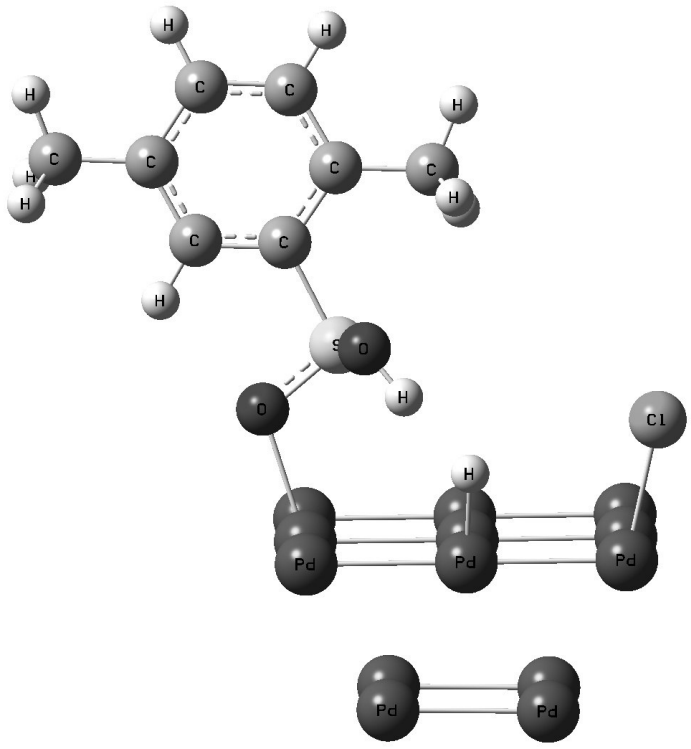


**Figure 4-11.** The calculated transition state structure over $Pd_{13}$. More specifically, this is the transition state for the conversion of 2,5-dimethylbezene sulfonyl chloride to 2,5-dimethylbenzene sulfinic acid and hydrochloric acid using $Pd_{13}$ as the simulated catalyst cluster. $E_a$ = -2.99 kcal/mol.

The calculated transition state using the $Pd_{13}$ cluster predicts a negative value for $E_a$. This is an impossible result, violating the scientific laws that apply in this situation. If not for the impossibly predicted $E_a$, however, the transition state does appear feasible. In fact it is very close in structure to the minimized product structure. Further, the application of the Hammond-Leffler Postulate[58] clears the picture even more. The Hammond-Leffler Postulate states that the structure of a transition state resembles that of the species nearest to it in free energy. That is to say that the transition state of an endothermic reaction resembles the products, while that of an exothermic reaction resembles the reactants. The overall reaction is exothermic ($\Delta H_{rxn}$ = -68 kcal/mol[2]) as is

the individual reaction step being simulated here ($\Delta H_{rxn}$ = -16.5 kcal/mol), thus the transition state structure should move along the reaction coordinate closer to the reactants of the reaction rather than the products.

The following procedure was followed. First, all molecules were locked into place in the calculated transition state structure. Next, to simulate moving along the reaction coordinate the hydrogen bound to the oxygen to form 2,5-dimethylbenzene sulfinic acid was freed and allowed to move along the 1.3 Å distance between its transition state location, forming the sulfinic acid, and its reactant location, forming the hydrogen molecule. This hydrogen was the only molecule allowed to move and single point energy calculations were performed at every 0.25 Å step to determine the change in enthalpy associated with that single atom moving. Table 4-2 summarizes the results.

**Table 4-2.** A summary of the effect on $E_a$ by moving the hydrogen atom. This table shows the data as discussed above when moving the hydrogen atom through the intervening distance between the product bond and the reactant bond.

| Simulation State | $E_a$ (kcal/mol) |
|---|---|
| Transition State | -2.99 |
| 1.9 Å | -2.63 |
| 1.65 Å | 8.28 |
| 1.40 Å | 25.76 |
| 1.15 Å | 34.87 |
| 0.90 Å | SCF Convergence Failure |
| 0.65 Å | SCF Convergence Failure |
| 0.6 Å (bound into H-H) | 62.69 |

Table 4-2 provided for even more confusion when viewed in light of the Hammond-Leffler Postulate. The position that would best match the experimental data for $E_a$ is very near to the minimized product structure in Figure 4-8. The calculated transition state structure is much closer to the product configuration than to the reactant configuration. Further, by moving the hydrogen atom somewhere between 0.25-0.5 Å away from the calculated transition state structure the $E_a$ results match those from experiments provided by DuPont. As the hydrogen atom moves closer to the reactant structure of molecular hydrogen, the calculations fail and cannot even provide a stable single-point energy calculation result.

A closer look was taken at the enthalpy change on reaction since the combination of the calculations and the experimental data pointed in a direction that was in direct contradiction to the Hammond-Leffler Postulate. If the Pd-adsorbed species from the previous section of this work are used to calculate the heat of reaction rather than the free gas species which were used in the calculation above, the hydrogenation of 2,5-dimethylbenzene sulfonyl chloride to 2,5-dimethylbenzene sulfinic acid is actually slightly endothermic ($\Delta H_{rxn}$ = +10 kcal/mol). This fact puts the calculation, the experimental data and the Hammond-Leffler Postulate all in agreement, the transition state should be closer to the product structure than the reactant structure. While the steep slope of the potential energy surface near the first-order saddle point corresponding to the transition state allowed the calculation to return a negative result, it can be easily

remedied to match experimental data by moving a single hydrogen atom by less than 0.5 Å.

A deeper investigation into the $Pd_{13}$ structure indicates that there are two possibilities. Either there is a very low energy barrier to overcome for reaction or, more likely, the structure calculated is actually an intermediate structure of a multi-step reaction process rather than the transition state of a single reaction.

**4.5 - Conclusions**

Using computational chemistry to determine transition states is problematic in the simplest of systems and here it was applied to a vastly complex reaction. Despite that, the results are within reason when compared to experimental values and the discrepancies between the calculations and the data can be explained. The work described herein provides a confirmation of the data received from DuPont that the first-order kinetics and proposed reaction system are most likely correct.

# 5. PLANT DESIGN AND ECONOMIC EVALUATION

## 5.1 - Introduction

Aromatic thiols are of industrial importance due to their use in the manufacture of agrochemicals, polymers, pigments, dyes and pharmaceuticals.[3,4] The particular case focused on here was the new technology for the reduction of aromatic sulfonyl chloride to the corresponding aromatic thiol. While this technology is patented[2] it is not yet commercialized. The purpose of this study is twofold. First, determine if the DuPont technology is a viable commercial option. Second, determine the specific challenges that would be faced by a group of engineering students performing design calculations on this reaction system. AspenTech[59] software for flowsheet design and ICARUS[60] software for economic analysis were used in addition to outside references when the computational options were insufficient to make progress. The end result is a better idea of the economic viability of the technology on the open market as well as a tested framework for engineering design students at Texas A&M to be introduced to aspects of design and economics in the specialty/fine chemicals arena.

*Reaction Description and Plant Design Procedure*

This work focused on the conversion of aromatic sulfonyl chloride to aromatic thiol, as shown in Figure 5-1.

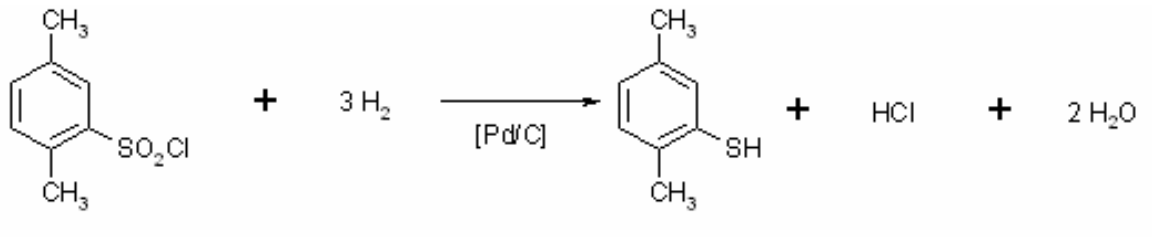


**Figure 5-1**. The overall sulfonyl chloride to thiol reaction. Any aromatic substitute can be used instead of the 2,5-dimethylbenzene group and still be accurate.

Preliminary work by DuPont indicated the overall conversion of the aromatic sulfonyl chloride could be represented by first order kinetics.[2] However, kinetics were not proposed for the secondary reactions. Figure 5-2 illustrates a probable stoichiometric reaction sequence that occurs on the path to production of an aromatic thiol. The proposed first order kinetics for the conversion of the aromatic sulfonyl chloride suggests that the adsorption of the sulfonyl chloride to the catalyst surface or the consumption of the sulfonyl chloride, shown in Figure 5-2, is the rate controlling step.

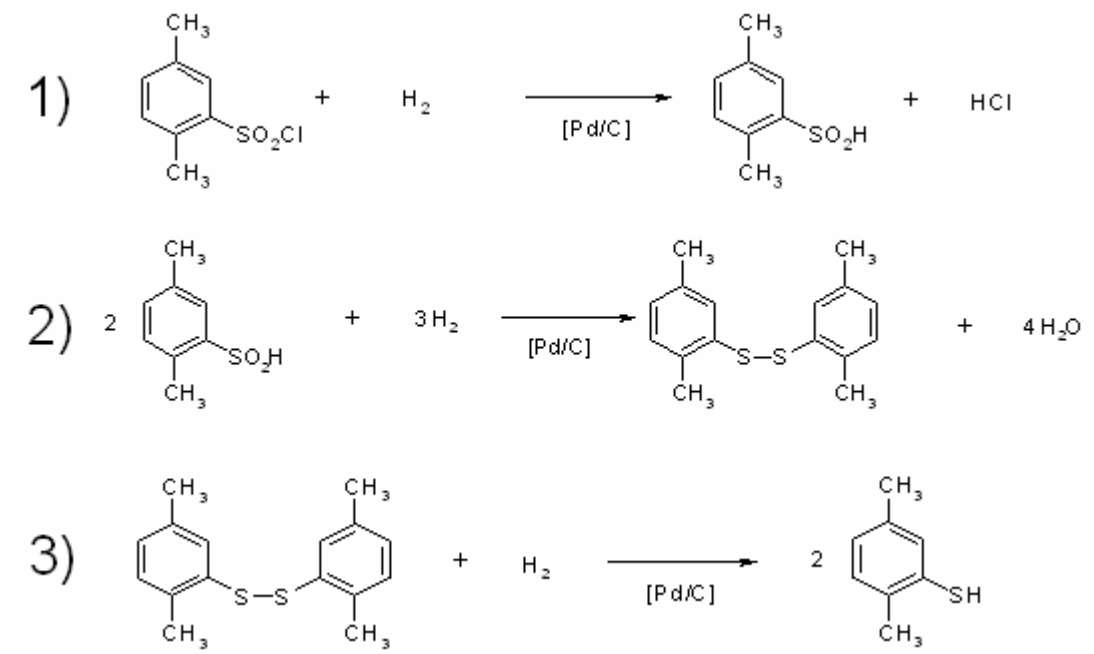


**Figure 5-2.** The steps of the overall reaction. No side product reactions are shown. Again, 2,5-dimethylbenzene may be substituted with any aromatic group.

This reaction performs optimally at pressures above 300 psi and temperatures above 100 C, though the Pd/C catalyst deactivates at temperatures above 125 C.[2] Reaction conditions were set at 300 psi and 110 C. In a batch reaction system the final product is a four-phase mixture of gas, solid, organic liquid and aqueous liquid which must be separated and either disposed of, in the cases of water and acidic wastes, recycled, in the cases of the Pd/C catalyst and hydrogen, or recovered, in the case of the thiol product. Additionally, the reaction is exothermic ($\Delta H_{rxn}$ = -63 kcal/mol sulfonyl chloride converted to thiol[2]), requiring cooling of some sort to be installed on a batch reactor to prevent runaway reactions.

Additional challenges come in satisfying software requirements for the design simulations. Experts state[61] that ASPEN converges with less difficulty when using molecular and thermodynamic properties from molecules already in its database rather than user-generated values or having the software estimate the parameters using its internal group contribution methods. Thus, with benzenethiol being a part of the ASPEN database and also the aromatic thiol with the highest levels of production commercially,[2] the design and economic analysis were performed on the production of benzenethiol rather than 2,5-dimethylbenzenethiol as shown above.

Further, the ASPEN software limitations are exceeded with this reaction as standard group contribution methods fail when calculating the sulfonyl chloride group. There were no experimental data available for benzenesulfonyl chloride and no database entry in ASPEN for it either. A new approach had to be taken. With ASPEN unable to handle the kinetics and thermodynamics of the sulfonyl chloride in the reaction, a two step approach was developed. The reactor was designed in a separate program, and then the calculated reactor product at the end of the reaction was fed into an ASPEN flowsheet that began with a flash tank to simulate the depressurization of the batch reactor to atmospheric pressure at the completion of the batch. From there ASPEN was used to determine and size the recovery train for the process and ICARUS was used to economically evaluate the cost of the system. The final result of this process will be a model of a 2 million lb/yr benzenethiol plant that can be used to determine the economic

feasibility of such a plant for presentations to customers that may be interested in purchasing the patented thiol technology.

## 5.2 - Reactor Design

*Construction Materials*

The hydrogenation reaction to produce benzenethiol also produces water and hydrochloric acid (HCl). At 110 C and 300 psi, the low pH environment generated during reaction is detrimental to the long term stability of common, carbon steel construction. Acid resistant materials must be used. Specialized alloys are normally cost prohibitive on reactors of great size and 25 years ago there would have been a call for doing the batch hydrogenation in a glass lined reactor. Glass-lined reactors are rarely used anymore, instead there is a trend towards Teflon-lined reactors, but there are several types of Teflon coatings to choose from.[62] Teflon PFA coated carbon steel was chosen as the construction material for the reactor. Teflon perfluoroalkoxy (PFA) non-stick coating was chosen because it gives a non-porous surface, is especially resistant to chemical processes and is the most versatile of the Teflon coating types. The coating's upper end operating temperature is 260 C, and it can be applied in layers up to a millimeter and is the most abrasion resistant and toughest of the non-stick polymers that can handle temperature in excess of 200 C. Also, the reactor will need to be agitated and have a cooling jacket.

*Reaction Requirements*

A 5000 gallon batch reactor constructed with materials as described above was chosen for the process. Toluene is to be used as a solvent for the reaction. Assuming that a reaction vessel should never be more than 80% liquid full because of safety concerns, the use of 3000 gal of solvent was chosen as the initial charge. This leaves room for the addition of reactants, catalysts and takes into account any possible volume change upon reaction. In their work[2] DuPont used a 25% by weight ratio of benzenesulfonyl chloride (BSCl) to toluene. Physical properties are presented in Table 5-1.

**Table 5-1**. The densities and molecular weights of all species involved in the reaction.[63]

| Compound Name | Density (g/cc) | Molecular Weight (g/mol) |
|---|---|---|
| Benzenesulfonyl Chloride (BSCl) | 1.294 | 204.6 |
| Benzenethiol | 1.02 | 138.23 |
| Toluene | 0.8669 | 92.14 |
| Water | 1.00 | 18 |
| HCl | 1.18 | 36.46 |
| Pd/C Catalyst | 0.55 | N/A |

Benzenesulfonyl chloride is a solid that is soluble in toluene. A 25% by weight solution of BSCl in toluene yields a solution containing just over 13000 moles of BSCl in 3000 gal of toluene. This solution is charged into the reactor. Catalyst is added to the reactor at a ratio of 0.013 lb catalyst/lb feed mixture. This accounts for 307 lbs of Pd/C catalyst per batch which adds 67 gal to the overall mixture, making the complete mixture 3545 gal. Pressurize the vessel to 300 psi with hydrogen gas and the reaction shown in Figure 5-1 will begin to take place even at room temperature. Since the reaction is exothermic

and the reactor is equipped with a water cooling jacket, calculations were run to determine how long the reaction would take to go to completion if allowed to use the reaction heat to heat the vessel rather than some artificial means of getting the reactor temperature to 110 C. The reactor contents were assumed to be 100% toluene for the purpose of calculating liquid heat capacity.

$$Cp_{liq} = A + BT + CT^2 + DT^3$$

Where,

$Cp_{liq}$ = The heat capacity of the reactor liquid, assumed to be equal to 100% toluene,

A = 83.073 J/mol-K,

B = 5.1666 x $10^{-1}$ J/mol-$K^2$,

C = -1.491 x $10^{-3}$ J/mol-$K^3$,

D = 1.9225 x $10^{-6}$ J/mol-$K^4$

and T = reactor temperature, K.

Changes within the reactor are governed by the equations and assumptions listed below.

$$k = A\exp\left[\frac{-Ea}{RT}\right]$$

Where,

k = reaction rate constant, $min^{-1}$,

A = Arrhenius constant, 1.92 x $10^7$ $min^{-1}$, [12]

$E_a$ = activation energy of the reaction, 14.58 kcal/mol, [12]

R = 1.9872 cal/mol K

and T = reaction temperature, K

From DuPont's proposed kinetics of first-order in the reactant:

$$\frac{-1}{V_{liq}}\frac{dn_{BSCl}}{dt} = kC_{BSCl}$$

Where,

t = time, min,

$C_{BSCl}$ = concentration of benzene sulfonyl chloride in the reaction mixture, mol/L,

$n_{BSCl}$ = number of moles of sulfonyl chloride, mol,

and $V_{liq}$ = the volume of the reactor liquid, total volume – catalyst volume, L.

With a simplifying assumption that the entirety of the reactor liquid will heat as only the solvent toluene, the following equation is used during the adiabatic operation of the reactor.

$$\frac{dT}{dt} = \frac{\Delta H_{rxn}}{mCp_{liq}}\left(\frac{dn_{BSCl}}{dt}\right)$$

Where,

T = reaction temperature, K,

$\Delta H_{rxn}$ = heat of reaction, -63 kcal/mol,

And m = total moles of toluene in reactor, mol.

And the equation below is used to determine the necessary heat transfer coefficient during isothermal operation.

$$Q = \left( \frac{dn_{BSCl}}{dt} \right) \Delta H_{rxn} = UA\Delta T$$

Where,

Q = heat load, W,

U = overall heat transfer coefficient for heat exchange, $W/m^2$-K

and A = surface area for heat exchange with reactor cooling jacket, $m^2$.

By using an ideal solution assumption:

$$\frac{dV_{liq}}{dt} = \left( -\frac{MW_{BSCl}}{\rho_{BSCl}} + \frac{MW_{HCl}}{\rho_{HCl}} + \frac{MW_{thiol}}{\rho_{thiol}} + \frac{2MW_{H_2O}}{\rho_{H_2O}} \right) \left( \frac{-dn_{BSCl}}{dt} \right)$$

Where,

$MW_i$ = molecular weight of component I, g/mol,

and $\rho_i$ = density of component i, g/cc.

$$X = \frac{n_{BSCl_0} - n_{BSCl}}{n_{BSCl_0}}$$

Where,

X = conversion, unitless,

and $n_{BSClo}$ = initial moles of benzenesulfonyl chloride.

Using the above equations along with an assumption of perfect mixing, adiabatic operation up to reaction temperature (110 C) and isothermal operation after that point, the solution to the system was determined using Euler's method. Heat transfer calculations showed that the jacketed reactor has enough cooling capacity to operate isothermally at reaction temperatures and peak reaction heat generation using room temperature water as a cooling fluid. Four different sized time steps were used and the results are summarized in Table 5-2 below.

**Table 5-2.** Results of the progression of the hydrogenation reaction. Data are presented over time given 4 different sized time steps. The reaction was considered complete when $n_{BSCl}/n_{BSClo}$ was less than $10^{-6}$.

| Step Size (min) | Time to Reaction Temperature (min) | Time for Reaction Completion (min) | Final Total Reaction Liquid Volume (gal) |
|---|---|---|---|
| 2 | 150 | 280 | 3765 |
| 1 | 147 | 284 | 3765 |
| 0.5 | 145 | 286 | 3765 |
| 0.1 | 144 | 287.4 | 3765 |

As presented in the Table 5-2, the reactor will arrive at the reaction temperature in approximately 2.5 hours and the ratio of $n_{BSCl}/n_{BSClo}$ will be less than $10^{-6}$ in less than 5 hours of reaction. As a conservative estimate, a batch reaction time of 7 hours, allowing for completion of the secondary reactions from the proposed reaction mechanism in Figure 5-2 and for more complete reaction, was chosen. A 7 hour reaction time also allows for a full reactor batch and 1 hour of turn-around time within a typical 8-hour work shift.

### 5.3 - Downstream Plant Design

The effluent stream from the reactor after a complete run will contain 192.46 lb mol of toluene, 28.888 lb mol of benzenethiol, 28.888 lb mol of HCl, 57.77 lb mol of water, the hydrogen used to pressurize the reactor, 307 lbs of catalyst solid (simulated as graphite) and trace amounts of benzenesulfonyl chloride at 300 psi and 110 C. This mixture is the inlet stream to the ASPEN simulation for design of the recovery process. The downstream processing equipment is sized to treat and recover the contents of one full reactor in one hour. The first step is to simulate the pressure release from the reactor at the end of a batch by putting the mixture through a simulated flash tank from 300 psi to atmospheric pressure. This first unit operation will provide data as to what components will need to be processed in the gas phase and which will be processed in the liquid phase. Since the benzenesulfonyl chloride is in trace amounts and ASPEN will not allow calculations to commence if it is included, assume that the effects of the benzenesulfonyl chloride are negligible and that it may be ignored throughout the downstream recovery calculations. The liquid and vapor streams from the flash tank are shown in Table 5-3.

**Table 5-3.** Calculated values of the liquid and vapor streams effluent from the reactor. These calculations were taken after depressurization from 300 psi to 14.7 psi.

| Component Name | Liquid Stream (lb mol) | Vapor Stream (lb mol) |
|---|---|---|
| Benzenethiol | 28.75 | 0.14 |
| Toluene | 171.55 | 20.91 |
| Water | 40.22 | 17.55 |
| Hydrochloric Acid | 0.25 | 28.64 |
| Hydrogen | 0.016 | 566.57 |
| Catalyst | All | None |

The initial flash calculation shows that, as expected, the hydrogen will leave in the vapor phase. Additionally, the vapor phase will take with it most of the HCl produced in the reaction leaving behind a relatively simple two step separation to recover the benzenethiol product. A separation of solids from liquids in the first step and a separation of aqueous and organic liquids in the second step will yield the benzenethiol in toluene solvent at a high purity. Solids must be recovered because of the expense of the Pd/C catalyst which will be recycled. The aqueous liquid phase from the liquid/liquid separator will carry away any additional acid left in the liquid. One additional processing step is needed before the aqueous waste can be sent to wastewater treatment. A deodorization step performed by mixing the aqueous phase from the liquid/liquid separator with a dilute solution of water and hypochlorite. Besides eliminating odors, the hypochlorite also neutralizes the remaining amount of HCl present in the aqueous phase. However, care must be taken not to bring the hypochlorite into contact with the benzenethiol as a reaction will occur between them and the product will disappear.

Gas processing is also necessary because of the huge amount of hydrogen that can be recycled and recovered. This will also be done in two steps using gas-liquid contacting columns. The first step will be a neutralization step where the effluent reactor vapor will be contacted with a 0.1 M solution of NaOH in water. This will effectively neutralize the HCl and prevent further corrosion due to acidic environments. Additionally, the resultant salty water is a candidate for sending to wastewater treatment. The second step is a combination deodorization/separation step accomplished by contacting the vapor from the first scrubber with a dilute solution of hypochlorite in water at a low temperature. This allows only the hydrogen to stay in the gas phase. The hydrogen is recycled to the front of the overall process while the liquid leaving the chilled column must be sent to the incinerator because the contents contain unknown organics from toluene and trace thiol remnants coming in contact with aqueous hypochlorite. The complete flowsheet from ASPEN is shown in Figure 5-3.

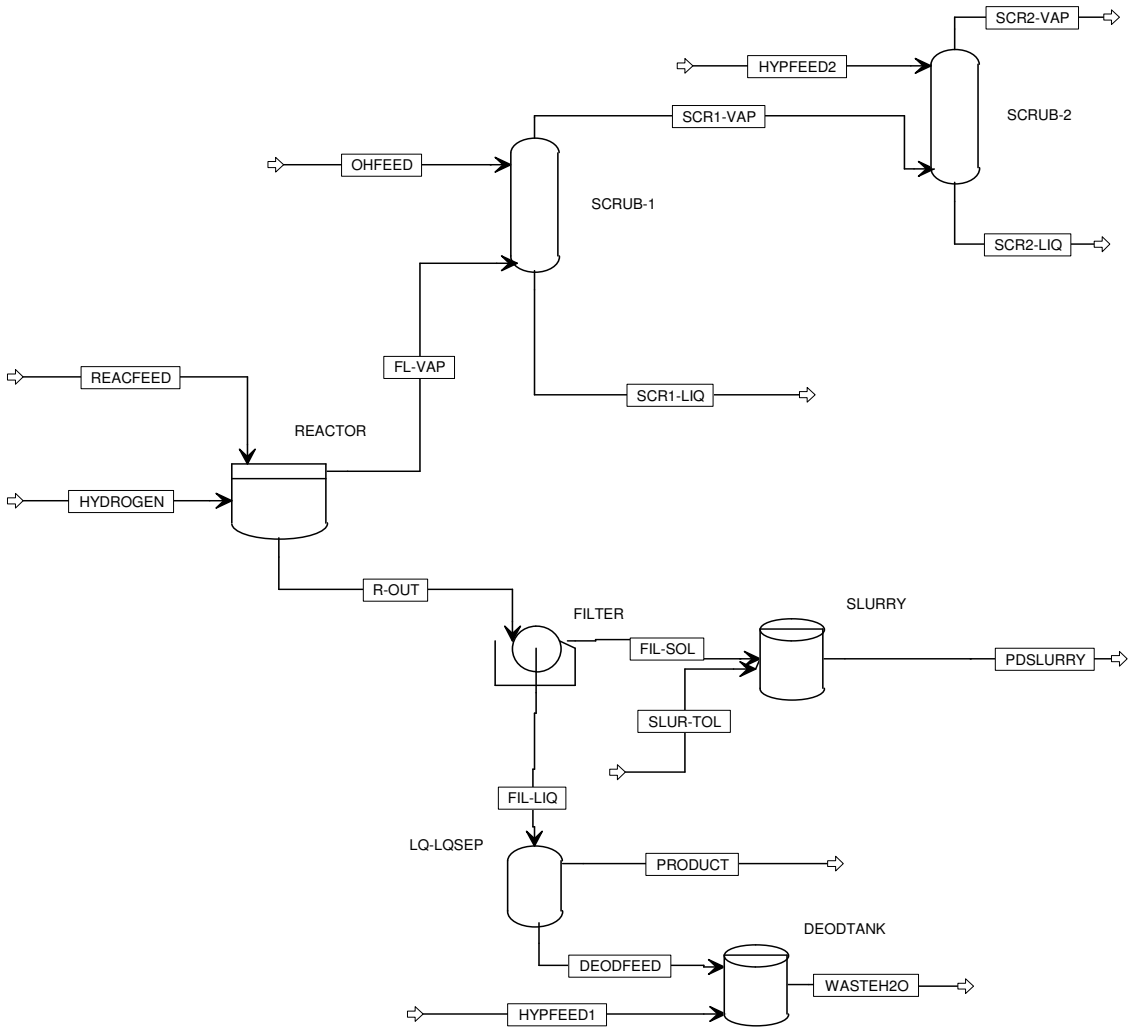


**Figure 5-3.** A flowsheet showing the benzenethiol hydrogenation process. The reactor is shown in its correct place though for calculation purposes it was a flash tank with a single inlet stream calculated by hand before ASPEN simulation. Recycle mechanisms for hydrogen and Pd/C catalyst are not shown.

## 5.4 - Process Description

*Hydrogenation Reactor*

The reactor, labeled REACTOR in Figure 5-3, is a 5000 gallon Teflon PFA coated carbon steel vessel complete with agitator and cooling water jacket. It will be run in a semi-batch mode with continuous hydrogen flow to keep the reactor pressure at 300 psi as the gas is consumed by the reaction. A single charge of ~3500 gallons of 25 wt% benzenesulfonyl chloride in toluene is loaded for each batch. In addition 307 lbs of Pd/C catalyst is charged for each batch. The reactor is allowed to use heat generated by the reaction to get the temperature up to 110 C where it will be held for the duration of the reaction time, 7 hours. After 7 hours, the pressure on the reactor is released and the contents are pumped to the downstream recovery operations of the process.

*Solids Processing*

The liquid-solid separator, labeled FILTER in Figure 5-3, is a standard rotary drum filter capable of separating 100% of liquid-borne solids with very little loss of liquid into the solids stream. According to calculations from ASPEN, more than 99.9% of the moles of benzenethiol processed through the filter were recovered in the liquid outlet stream while none of the catalyst was lost. The catalyst continues onward from the rotary drum filter via conveyor to be placed into an agitated slurry tank, labeled SLURRY in Figure 5-3, where it is combined into a 2:1 toluene to catalyst slurry to be recycled to the front of the hydrogenation process.

*Liquid-Liquid Separation and Product Recovery*

The liquid recovered from the rotary filter continues to a simple settling tank, labeled LQ-LQSEP in Figure 5-3, allowing the two distinct organic and aqueous phases to separate and be pumped away separately. The aqueous phase off the bottom is sent to an agitated tank, labeled DEODTANK in Figure 5-3, where it is mixed with a dilute aqueous solution of hypochlorite for deodorization and neutralization purposes. It is then sent to wastewater treatment. The organic phase off the top of the recovery tank is a stream of benzenethiol in a solution of toluene. The amount of recovered benzenethiol is 99.91% of the total product that was effluent from the reactor. The total yield in this ideal case for economic feasibility studies is 3970 lbs benzenethiol/batch. The process will produce 2 million pounds of benzenethiol in 504 batches. That is running two 8 hour (counting turnaround time) batches a day for 252 working days, far short of normal expectations of 24 hour operation for 300 days a year. On a global scale, 2 million pounds of benzenethiol translates into an immediate 18% total market share since total worldwide production capacity at this point is only 10 million lbs/yr.[2]

*Gas Processing*

Gas processing is performed in two gas-liquid contact steps. The first is a neutralization step in a large contactor column, labeled SCRUB-1 in Figure 5-3, where the reactor effluent gas comes into contact with 10000 lbs of a 0.1 M solution of NaOH in water to neutralize the HCl that exits the reactor. Nearly all of the HCl produced during the hydrogenation reaction (99.14%) comes through this neutralization column; the other

0.86% is the small amount in the aqueous liquid phase on the product recovery/liquid processing side of the process. The solution of NaOH is in excess to neutralize the HCl, thus only very small amounts are in the exit liquid from the neutralization column and none is in the exit vapor. The exit vapor from the neutralization column is 94.4 mol% hydrogen with the remainder being about half toluene and half water with traces of the thiol still remaining. The exit vapor must undergo a deodorization step and the hydrogen needs to be recovered. These steps are performed simultaneously in the deodorization column, labeled SCRUB-2 in Figure 5-3. SCRUB-2 is a chilled column and a gas-liquid contactor for the SCRUB-1 exit vapor stream and a dilute solution of aqueous hypochlorite, which will neutralize the thiol odors. Only hydrogen with trace amounts of water and toluene exits in the SCRUB-2 vapor stream. This stream is recycled to the front of the process to reduce costs. The organic/aqueous mixture that flows out of the liquid stream from the deodorization column is safer to simply incinerate because of the unknown mixture of organic compounds created by contacting toluene and trace amounts of benzenethiol with the hypochlorite.

**5.5 - Economic Analysis**

An initial assumption must be made to make further calculations possible. The assumption is that the sudden construction of a plant to take an immediate 18% world market share on the production of benzenethiol will not affect worldwide prices. This assumption is obviously flawed, but it allows the in depth economic process analysis to be completed. The results from the ASPEN flowsheet for the recovery and recycling

equipment were put into ICARUS for equipment costing purposes only. Those results and the values determined through charts in Peters and Timmerhaus for the reactor and the storage tanks, which were not simulated in ASPEN, are presented in Table 5-4.

**Table 5-4.** Equipment cost listed by piece of equipment and source of the data.

| Unit Operation | Purchased Equipment Cost | Data Source |
|---|---|---|
| Reactor | $354,000 | Peters/Timmerhaus[64] |
| Rotary Filter | $54,000 | ICARUS |
| Liq-Liq Separator | $11,200 | ICARUS |
| Scrub 1 Tower | $60,400 | ICARUS |
| Scrub 2 Tower | $43,300 | ICARUS |
| 7 Storage Tanks | $332,500 | Peters/Timmerhaus |

Each of the 7 storage tanks is calculated as a 10000 gallon, stainless steel tank with agitator. Table 5-4 shows a total equipment cost of $855,400. This amount can then be used in a standard table given in Peters and Timmerhaus[64] to give the results that are shown in Table 5-5.

**Table 5- 5.** The results of the costing of the full equipment list. Data were compiled using a table from Peters and Timmerhaus. The table provides percentage ranges for each component of the total capital investment. Once the values of each percentage have been chosen (median values were used in this case) they can each be determined from the previously totaled purchased equipment cost. The total fixed capital investment is calculated by summing the individual parts.

| Component | % of Total | Capital Cost | |
|---|---|---|---|
| Purchased Equipment | 25 | $855,400 | |
| Installation | 9 | $307,944 | |
| Instrumentation (Installed) | 7 | $239,512 | |
| Piping (Installed) | 8 | $273,728 | |
| Electrical (Installed) | 5 | $171,080 | |
| Buildings (including Service) | 5 | $171,080 | |
| Yard Improvements | 2 | $68,432 | |
| Service Facilities (Installed) | 15 | $513,240 | |
| Land | 1 | $34,216 | |
| Engineering and Supervision | 10 | $342,160 | |
| Construction Expense | 12 | $410,592 | |
| Contractor's Fee | 2 | $68,432 | |
| Contingency | 8 | $273,728 | |
| | | $3,729,544 | **Total Fixed Capital Investment** |

The total fixed capital investment is the most important number in economic feasibility studies. This is the value that the company must recoup through sales of benzenethiol product.

Most companies use some level of measure for how quickly a given process will pay back its initial investment and start turning a profit for the company. In this study, a payback time calculation will be performed and compared to a value of 3-4 years to payback. This commonly used value varies from company to company across the world, but 3-4 years for payback is widely held as a minimum number for economic feasibility.

Two separate scenarios were used for the calculation under consideration. One is a plant built on the Gulf Coast of the US, the other is a plant built in the Chinese or SE Asian marketplace with their cheaper, but skilled labor force providing a cost advantage. The results are tabulated below in Tables 5-6 and 5-7 respectively. When applicable, the Tables below used the MACRS 3 yr depreciation system as it the most aggressive covered in the texts. A standard rate of 33% income tax was used in all examples. Cost of manufacture (COM) is defined as the sum of raw material costs and operating costs. Cost of sales (COS) is defined as 1.4 x COM to account for advertising, sales and general marketing expenses. The selling price of $2.27/lb benzenethiol is current as of the summer of 2007.

**Table 5-6.** A summary of the economic feasibility of a 2 million lb/yr benezenethiol plant built on the Gulf Coast of the US.

| Gulf Coast Option | $600k/yr Operators | |
|---|---|---|
| Operating Costs | $1,170,000.00 | $/yr |
| Raw Material Costs | $1.05 | $/lb thiol |
| Operating Costs | $0.59 | $/lb thiol |
| Cost of Manufacture | $1.64 | $/lb thiol |
| Cost of Sales | $2.29 | $/lb thiol |
| Selling Price | $2.27 | $/lb thiol |
| Pretax Profit | -$49,200.00 | $/yr |
| | | |
| No Profit to be made here | Payback time is infinite | |

**Table 5-7.** A summary of the economic feasibility of a 2 million lb/yr benezenethiol plant built in the Chinese or SE Asian markets.

| China/SE Asia Option | $150k/yr Operators | |
|---|---|---|
| Operating Costs | $720,000.00 | $/yr |
| Raw Material Costs | $1.05 | $/lb thiol |
| Operating Costs | $0.36 | $/lb thiol |
| Cost of Manufacture | $1.41 | $/lb thiol |
| Cost of Sales | $1.98 | $/lb thiol |
| Selling Price | $2.27 | $/lb thiol |
| Pretax Profit | $580,800.00 | $/yr |
| Post Tax Profit | $389,136.00 | $/yr |
| MACRS 3yr system | $285,104.82 | $ in Yr1 |
| | $380,225.30 | $ in Yr2 |
| | $126,684.74 | $ in Yr3 |
| | $63,385.14 | $ in Yr4 |
| | | |
| Payback Money | $674,240.82 | Year 1 |
| | $769,361.30 | Year 2 |
| | $411,789.56 | Year 3 |
| | $443,610.44 | Year 4 |
| | $389,136.00 | Year 5+ |
| | | |
| Total Payback Time | 7.67 years | |

As Tables 5-6 and 5-7 show, the economic feasibility for the DuPont thiol technology is poor. A plant on the Gulf Coast of the US actually loses $0.02/lb thiol produced in this simulation. While the more competitive Asian markets can at least turn a profit, it still takes more than 7.5 years to pay back the initial capital investment. By delving deeper into the costs associated with the hydrogenation process, the biggest single expense item is the cost of the benzenesulfonyl chloride reactant. The calculations performed above assumed paying market value for the reactant which in itself is an expensive, specialty commodity chemical. Many companies can achieve a cost advantage on sulfonyl chloride reactants if they are already in the thiol-producing business by either producing sulfonyl chloride themselves from cheaper raw materials or by signing lucrative bulk contracts in partnership with other businesses. A third calculation was performed assuming a 25% cost savings versus market value on the benzenesulfonyl chloride cost in the Asian market to determine what gains could be made. The results are shown below in Table 5-8.

**Table 5-8.** A summary of the economic feasibility of a 2 million lb/yr benezenethiol plant built in the Chinese or SE Asian markets. Incorporated in this study was a 25% savings on the cost of the benzenesulfonyl chloride reactant.

| China/SE Asia Option | $150k/yr Operators | |
|---|---|---|
| Operating Costs | $720,000.00 | $/yr |
| Raw Material Costs | $0.85 | $/lb thiol |
| Operating Costs | $0.36 | $/lb thiol |
| Cost of Manufacture | $1.21 | $/lb thiol |
| Cost of Sales | $1.69 | $/lb thiol |
| Selling Price | $2.27 | $/lb thiol |
| Pretax Profit | $1,161,800.00 | $/yr |
| Post Tax Profit | $778,406.00 | $/yr |
| MACRS 3yr system | $285,104.82 | $ in Yr1 |
| | $380,225.30 | $ in Yr2 |
| | $126,684.74 | $ in Yr3 |
| | $63,385.14 | $ in Yr4 |
| | | |
| Payback Money | $1,063,510.82 | Year 1 |
| | $1,158,631.30 | Year 2 |
| | $905,090.74 | Year 3 |
| | $841,791.14 | Year 4 |
| | $778,406.00 | Year 5+ |
| | | |
| Total Payback Time | 3.715 years | |

The discount brings the economics of the Asian plant for the hydrogenation into a range where it may be considered a commercially viable process. Incidentally, the US plant with a 25% savings shows a payback time of 8.07 years. That value is still outside of the realm of economic feasibility, but it is turning a profit rather than losing money like the first example showed.

### 5.6 - Conclusion

This study set out to investigate the economic feasibility of a novel, aromatic thiol production technology and to set up a framework within which future engineering design students may learn about fine/specialty chemical manufacture. Through the work in this study the framework has been partially built for those future students to work with the kinetics and thermodynamics involved in this specific hydrogenation plant. Unfortunately, only direct, involved experimentation on sulfonyl chloride components will yield suitable thermodynamic data to allow ASPEN to handle the reaction/reactor portion of this system as easily as it does those utilizing only ASPEN database compounds. However, the economic analyses performed provide insight on the challenges faced by US manufacturers of fine/specialty chemicals when confronted by a worldwide marketplace. These facts can easily be introduced in a classroom setting giving students a wider view of the chemical industry. As for the economic feasibility of the process, according to the calculations performed herein, unless a company has the competitive advantages of access to a skilled work force on the pay scales of those in Asian markets and also has a way to get a discounted rate on raw materials involved in the hydrogenation, this process is not feasible to use as a grassroots plant construction process at the market price of $2.27/lb of benzenethiol reported in the summer of 2007.

# 6. CONCLUSION

The novel, green aromatic thiol production technology worked out. Quantum mechanical simulations have shown that the proposed reaction sequence from DuPont is a feasible representation of the process at a molecular level and that in the case of the first reaction steps the molecules move to favorable structures for reaction progression. The QM calculations have also disproved an alternate reaction pathway that was proposed based on molecular observations during the course of the simulations. Design and economic calculations have shown that without a very cheap, skilled labor force in addition to a means for a substantial savings on certain raw material costs, the thiol production technology is not economically desirable enough for companies to invest in a grassroots plant construction. However, those same calculations have pinpointed the areas of the process on which further study can be performed to help make the patented technology a more commercially viable option. The technology does require further development.

## REFERENCES

[1] P. T. Anastas, J. C. Warner, Green Chemistry Theory and Practice, Oxford University Press, New York, 1998.

[2] S. E. Jacobson, E. I. Du Pont De Nemours and Company. International Publication Number: WO 01/66517 A1, World Intellectual Property Organization, International Bureau, September 13 2001. Included in this reference are additional proprietary data and reports received by Texas A&M University from DuPont during the technology donation process.

[3] K. M. Roy, Ullman's Encyclopedia of Industrial Chemistry, Wiley-VCH, New York, 2003.

[4] J. S. Roberts, Encyclopedia of Chemical Technology, Vol. 24, John Wiley and Sons, New York, 1997.

[5] M. Hudlický, Reductions in Organic Chemistry, 2nd ed., American Chemical Society, Washington DC, 1996.

[6] H. Gilman, A. H. Blatt, Organic Syntheses. Collective Volume I, John Wiley and Sons, New York, 1941.

[7] H. Gilman, A. H. Blatt, Organic Synthesis: Collective Volume I, 2nd ed., John Wiley and Sons, Inc., New York, 1948.

[8] H. A. Bent, W. W. Brand, L. Field, E. T. Kaiser, T. C. Klingler, N. Kunieda, R. Mayer, S. Oae, A. Ohno, M. Porter, C. J. M. Stirling, W. Tagaki, W. E. Truce, Organic Chemistry of Sulfur, Plenum Press, New York, 1977.

[9] J. S. Poland, S. Mitchell, A. Rutter, Cold Reg. Sci. Technol., 32 (2001) 93.

[10] S. L. Bruce, B. N. Noller, A. H. Grigg, B. F. Mullen, D. R. Mulligan, P. J. Ritchie, N. Currey, J. C. Ng, Toxicol. Lett., 137 (2003) 23.

[11] F. Piao, K. Yokoyama, N. Ma, T. Yamauchi, Toxicol. Lett., 145 (2003) 28.

[12] B. Zerahn, A. Kofoed-Enevoldsen, B. V. Jensen, J. Mølvig, N. Ebbehøj, J. Johansen, I.-L. Kanstrup, Resp. Med., 93 (1999) 885.

[13] R. L. White, Basic Quantum Mechanics, McGraw Hill Book Co., New York, 1966.

[14] A. Szabo, N. S. Ostlund, Modern Quantum Chemistry, Dover Publications Inc., Mineola, NY, 1989.

[15] B. T. Sutcliffe, Computational Techniques in Quantum Chemistry, Reidel, Boston, 1975.

[16] M. J. Frisch, G. W. Trucks, H. B. Schlegel, G. E. Scuseria, M. A. Robb, J. R. Cheeseman, J. A. Montgomery, Jr., T. Vreven, K. N. Kudin, J. C. Burant, J. M. Millam, S. S. Iyengar, J. Tomasi, V. Barone, B. Mennucci, M. Cossi, G. Scalmani, N. Rega, G. A. Petersson, H. Nakatsuji, M. Hada, M. Ehara, K. Toyota, R. Fukuda, J. Hasegawa, M. Ishida, T. Nakajima, Y. Honda, O. Kitao, H. Nakai, M. Klene, X. Li, J. E. Knox, H. P. Hratchian, J. B. Cross, C. Adamo, J. Jaramillo, R. Gomperts, R. E. Stratmann, O. Yazyev, A. J. Austin, R. Cammi, C. Pomelli, J. W. Ochterski, P. Y. Ayala, K. Morokuma, G. A. Voth, P. Salvador, J. J. Dannenberg, V. G. Zakrzewski, S. Dapprich, A. D. Daniels, M. C. Strain, O. Farkas, D. K. Malick, A. D. Rabuck, K. Raghavachari, J. B. Foresman, J. V. Ortiz, Q. Cui, A. G. Baboul, S. Clifford, J. Cioslowski, B. B. Stefanov, G. Liu, A. Liashenko, P. Piskorz, I . Komaromi, R. L. Martin, D. J. Fox, T. Keith, M. A. Al-Laham, C. Y. Peng, A. Nanayakkara, M. Challacombe, P. M. Gill, B. Johnson, W. Chen, M. W. Wong, C. Gonzalez, J. A. Pople, Gaussian 03, Revision C.02, Gaussian, Inc., Wallingford CT, 2004.

[17] Wikipedia, Basis Set (Chemistry), http://en.wikipedia.org/wiki/Basis_set_%28chemistry%29, last visited March 2008.

[18] Wikipedia, Gaussian Orbitals, http://en.wikipedia.org/wiki/Gaussian_orbitals, last visited March 2008.

[19] A. D. Becke, J. Chem. Phys., 98 (1993) 5648.

[20] C. Lee, W. Yang, R. G. Parr, Phys. Rev. B., 37 (1988) 785.

[21] G. Barone, D. Duca, J. Mol. Struct.-Theochem, 584 (2002) 211.

[22] G. Barone, D. Duca, J.Catal., 211 (2002) 296.

[23] G. Barone, D. Duca, Chem. Eng. J., 91 (2003) 133.

[24] D. Duca, G. Barone, Z. Varga, G. La Manna, J. Mol. Struct.-Theochem, 542 (2001) 207.

[25] G. La Manna, G. Barone, Z. Varga, D. Duca, J. Mol. Struct.-Theochem, 548 (2001) 173.

[26] V. Pallassana, M. Neurock, Chem. Eng. Sci., 54 (1999) 3423.

[27] M. Neurock, S. A. Wasileski, D. Mei, Chem. Eng. Sci., 59 (2004) 4703.

[28] R. Hirschl, A. Eichler, J. Hafner, J. Catal., 226 (2004) 273.

[29] V. Bertani, C. Cavallotti, M. Masi, S. Carrà, J. Mol. Catal. A-Chem., 204-205 (2003) 771.

[30] A. Vargas, T. Burgi, A. Baiker, J. Catal., 222 (2004) 439.

[31] A. Vargas, T. Burgi, A. Baiker, J. Catal., 226 (2004) 69.

[32] I. Efremenko, M. Sheintuch, J. Mol. Catal. A-Chem., 160 (2000) 445.

[33] I. Efremenko, J. Mol. Catal. A-Chem., 173 (2001) 19.

[34] I. Efremenko, M. Sheintuch, J. Catal., 214 (2003) 53.

[35] I. Efremenko, M. Shientuch, Surf. Sci., 414 (1998) 148.

[36] R. Ishiwatari, M. Tachikawa, J. Mol. Struct., 735-736 (2005) 383.

[37] Gale Group, Chem. Week, 169(7) (2007) 16.

[38] S. Avery, Purchasing, 136(7) (2007) 32C9.

[39] CNCIC Chemdata Co. Ltd.; China Chem. Rept., 18(11) (2007) 25.

[40] Gale Group; Chem. Week, 169(20) (2007) 25.

[41] Conversations with Dr. Ed Mahler, E. I. DuPont and Co., Spring 2007.

[42] W. T. Tsai, H. P. Chen, W. Y. Hsien, C. W. Lai, M. S. Lee, Resour. Conserv. Recy., 39 (2003) 65.

[43] P. J. Hay, W. R. Wadt, J. Chem. Phys., 82 (1985) 270.

[44] Y. Wang, Z. Cao, Q. Zhang, Chem. Phys. Lett., 376 (2003) 96.

[45] B. N. Gogoi, A. Hargreaves, Acta Cryst., B26 (1970) 2132.

[46] L. Párkányi, G. Besenyei, J. Mol. Struct., 691 (2004) 97.

[47] R. Haist, F. Trautner, J. Mohtasham, R. Winter, G. L. Gard, H. Oberhammer, J. Mol. Struct., 550-551 (2000) 59.

[48] P. A.Gravil, H. Toulhoat, Surf. Sci., 430 (1999) 176.

[49] E. K. Poels, W. P. van Beek, W. den Hoed, C. Visser, Fuel, 74 (1995) 1800.

[50] C. H. Bartholomew, Appl. Catal. A-Gen., 212 (2001) 17.

[51] Z. Paál, K. Matusek, M. Muhler, Appl. Catal. A-Gen., 149 (1997) 113.

[52] D. R. Alfonso, A. V. Cugini, D. S. Sholl, Surf. Sci., 546 (2003) 12.

[53] K. Hansen, Š. Højrup, E. Lægsgaard, F. Besenbacher, I. Stensgaard, Surf. Sci., 505 (2002) 25.

[54] Y. Cao, Z.-X. Chen, Surf. Sci., 600 (2006) 4572.

[55] L. L. Jewell, B. H. Davis, Appl. Catal. A-Gen., 310 (2006) 1.

[56] E. K. Novakova, L. McLaughlin, R. Burch, P. Crawford, K. Griffin, C. Hardacre, P. Hu, D. W. Rooney, J. Catal., 249 (2007) 93.

[57] Wikipedia, Transition State, http://en.wikipedia.org/wiki/Transition_state, last visited March 2008.

[58] G. S. Hammond, J. Am. Chem. Soc., 77 (1955) 334.

[59] Aspen Technology Inc., Aspen Plus, aspenONE version 2004.1[13.2.0.2925], built April 5, 2005.

[60] Aspen Technology Inc., Aspen Icarus Process Evaluator, aspenONE software version 2004.2[14.0.1725], built October 11, 2005.

[61] Conversations with Ben Cormier, Dr. John Baldwin and Dr. Mahmoud El-Halwagi of the Artie McFerrin Department of Chemical Engineering at Texas A&M University, Spring 2007.

[62] E. I. DuPont and Co., DuPont Teflon Product Information Website, http://www2.dupont.com/Teflon_Industrial/en_US/products/selection_guides/coatings.html, last visited March 2008.

[63] Hazard.com SIRI MSDS Website, http://www2.hazard.com/msds/index.php, CAS Nos.: 7732-18-5; 7647-01-0; 108-88-3; 108-98-5; 98-09-9, last visited March 2008.

[64] M. S. Peters, K. D. Timmerhaus, Plant Design and Economics for Chemical Engineers, McGraw-Hill Inc., New York, 1991.

# VITA


Name: Bradley Ruston Atkinson

Address: PO Box 575 Warren TX, 77664

Email Address: mestifo@yahoo.com


Education: B.S., Chemical Engineering, University of Arkansas, 1998
M.S., Chemical Engineering, University of Arkansas, 2001
Ph. D. Chemical Engineering, Texas A&M University, 2008

Publications: Fluorescent Virus Use in Membrane Testing, University of Arkansas Press (Master's Thesis), 2001

Presentations: Investigation into a Novel, Green Technology for Aromatic Thiol Production, 10th Topical Conference on Refinery Processing, 2007 AIChE Spring National Meeting, Houston TX

Investigation into a Novel, Green Technology for Aromatic Thiol Production, 9th Topical Conference on Refinery Processing, 2006 AIChE Spring National Meeting, Orlando FL